IEEE Access
Multidisciplinary | Rapid Review | Open Access Journal

Received February 5, 2021, accepted February 15, 2021, date of publication February 19, 2021, date of current version March 4, 2021.

Digital Object Identifier 10.1109/ACCESS.2021.3060431

An Effective Salp Swarm Based MPPT for Photovoltaic Systems Under Dynamic and Partial Shading Conditions

MOHD NASRUL IZZANI JAMALUDIN[1], MOHAMMAD FARIDUN NAIM TAJUDDIN[1], JUBAER AHMED[2], (Member, IEEE), AZRALMUKMIN AZMI[1], (Member, IEEE), SYAHRUL ASHIKIN AZMI[1], NUR HAFIZAH GHAZALI[3], (Member, IEEE), THANIKANTI SUDHAKAR BABU[4], (Senior Member, IEEE), AND HASSAN HAES ALHELOU[5,6], (Senior Member, IEEE)

[1]Faculty of Electrical Engineering Technology, Universiti Malaysia Perlis, Arau 01000, Malaysia
[2]Swinburne University of Technology Sarawak, Kuching 93350, Malaysia
[3]Faculty of Electronic Engineering Technology, Universiti Malaysia Perlis, Arau 02600, Malaysia
[4]Department of Electrical and Electronics Engineering, Chaitanya Bharathi Institute of Technology (CBIT), Hyderabad 500075, India
[5]School of Electrical and Electronic Engineering, University College Dublin, Dublin 4, Ireland
[6]Department of Electrical Power Engineering, Faculty of Mechanical and Electrical Engineering, Tishreen University, Lattakia 2230, Syria

Corresponding authors: Hassan Haes Alhelou (alhelou@ieee.org) and Thanikanti Sudhakar Babu (sudhakarbabu66@gmail.com)

This work was supported in part by the Universiti Malaysia Perlis, and in part by the Ministry of Education (MOE), Malaysia, for providing the facilities through the Fundamental Research Grant Scheme (FRGS) under Grant FRGS/1/2018/TK07/UNIMAP/02/1. The work of Hassan Haes Alhelou was supported in part by the Science Foundation Ireland (SFI) through the SFI Strategic Partnership Programme under Grant SFI/15/SPP/E3125, and in part by the UCD Energy Institute.

ABSTRACT This study proposes a duty cycle-based direct search method that capitalizes on a bioinspired optimization algorithm known as the salp swarm algorithm (SSA). The goal is to improve the tracking capability of the maximum power point (MPP) controller for optimum power extraction from a photovoltaic system under dynamic environmental conditions. The performance of the proposed SSA is tested under a transition between uniform irradiances and a transition between partial shading (PS) conditions with a focus on convergence speed, fast and accurate tracking, reduce high initial exploration oscillation, and low steady-state oscillation at MPP. Simulation results demonstrate the superiority of the proposed SSA algorithm in terms of tracking performance. The performance of the SSA method is better than the conventional (hill-climbing) and among other popular metaheuristic methods. Further validation of the SSA performance is conducted via experimental studies involving a DC-DC buck-boost converter driven by TMS320F28335 DSP on the Texas Instruments Experimenter Kit platform. Hardware results show that the proposed SSA method aligns with the simulation in terms of fast-tracking, convergence speed, and satisfactory accuracy under PS and dynamic conditions. The proposed SSA method tracks maximum power with high efficiency through its superficial structures and concepts, as well as its easy implementation. Moreover, the SSA maintains a steady-state oscillation at a minimum level to improve the overall energy yield. It thus compensates for the shortcomings of other existing methods.

INDEX TERMS MPPT, salp swarm optimization, partial shading, PV characteristic, MATLAB.

I. INTRODUCTION

Over the past decade, the increasing energy consumption and the inevitable reduction in fossil fuel resources (coal, oil, natural gas), as well as the rapid environmental deterioration resulting from global warming, have prompted global efforts to study renewable energy sources (RESs), such as wind, solar energy, hydropower, geothermal energy and biomass [1]. Overcoming these issues has become the focus of global market interest. Also, power generation from RESs saves billions of barrels of crude oil and reduces carbon dioxide (CO_2) emissions and greenhouse gases [2], [3].

The associate editor coordinating the review of this manuscript and approving it for publication was Arash Asrari.

Solar energy is a pure form of energy directly from the sun. It is considered a state-of-the-art RES for electricity generation basically because solar energy is harmless to the environment. The sun's energy is a thousand times greater than the energy produced by fossil fuels in one day [4]. Another benefit of solar energy is that it can be used by virtually almost every country to produce electricity without depending on other nations. As solar energy is eternal and continuing, its long-term use can be guaranteed.

Solar photovoltaic (PV) is one of the world's most promising and abundant RESs. PV systems are clean, durable, noise-free, freely available, and omnipresent. Additionally, they are free from rotating parts, and they do not require heavy maintenance. These systems are also used in various applications, such as road lighting, solar cars, and hybrid renewable energy systems. According to International Energy Agency reports, the global primary energy utilization demand will increase by 60% from 2002 to 2030 [5], and PV systems will produce around 11% of the world's electricity and avoid 2.3 Gt of CO_2 emissions per year by 2050 [6]. After hydropower and wind, PV has become the third most important source of renewable energy. The International Energy Agency for Photovoltaic Power Systems reports that the global installation of PV capacity expanded to 227 GW in March 2015 and is expected to reach 500 GW by the end of 2020 [7].

NOMENCLATURE

D	Duty cycle
PV	Photovoltaic
MPP	Maximum power point
$GMPP$	Global maximum power point
$LMPP$	Local maximum power point
GP	Global peak
I_{SC}	Short circuit current
V_{OC}	Voltage open circuit
I_{MPP}	Current at maximum power point
V_{MPP}	Voltage at maximum power point
P_{MPP}	Power at maximum power point
V_{PV}	Tracked PV voltage
I_{PV}	Tracked PV current
C_1	Coefficient parameter
C_2, C_3	Random number
ub	Upper boundary
lb	Lower boundary
F	Food source
P_o	Output power
f_S	Switching frequency
L_1	Inductor
ΔP	Power differential ratio
$\Delta V_o/V_o$	Voltage ripple
η_{mppt}	MPPT efficiency
V_o	Initial speed
t	Time
a	Acceleration
d_i^k	Initial duty cycle
$GBest$	Global best position
L	Maximum iteration
l	Current iteration
$P_i^{(k)}$	Current at i-th iteration
$P_i^{(k-1)}$	Power at i-1th iteration
LP	Local peak
PS	Partial shading conditions

However, PV systems' power generation remains uncertain because of the low-efficiency yield resulting from varying environmental conditions, such as partial shading (PS) and irradiance conditions [8], [9]. The characteristics of a nonlinear PV source vary depending on the solar irradiance and temperature received. The occurrence of partial shading conditions (PSCs) causes the power vs. voltage (P-V) characteristic curve to become multimodal [10]–[13]. Hence, PV systems are equipped with maximum power point trackers (MPPTs) to ensure optimum energy extraction from PV arrays and thereby overcome the aforementioned problems. However, existing conventional MPPT algorithms [14]–[19] cannot differentiate local and global maximum points and thus have low effectiveness, particularly in dealing with multiple peaks problems. The ideal MPPT should track the actual maximum power point (MPP) for all environmental situations, including PSCs.

Numerous MPPT techniques have been introduced in the literature. They can be classified into two major classes, namely, conventional and metaheuristic algorithms. Conventional algorithms include perturb and observe (P&O) [20], which was previously referred to as hill climbing (HC) [21], incremental conductance [22], ripple correlation control [23], and extremum seeking control [24]. Metaheuristic algorithms include artificial intelligence (AI) and evolutionary computation (EC). AI consists of fuzzy logic [25] and artificial neural networks [26], [27]. EC includes the genetic algorithm (GA) [28], particle swarm optimisation (PSO) [29], [30], cuckoo search (CS) [31], fractional chaotic FPA [32], flow regime algorithm, social mimic optimization, Rao algorithm, ant colony optimisation (ACO) [33], [34], butterfly optimization algorithm [35], [36], grasshopper optimization algorithm [37], bat algorithm [38], metaphor-less algorithms [39] and many more.

Under uniform conditions, conventional MPPT techniques, such as HC, can track the global MPP on the I-V curve, but they fail to track the global MPP under PSCs. This phenomenon (PSC) occurs when the PV modules in a PV array panel do not receive uniform irradiance. It could also be due to obstacles (buildings, telephone poles, electrical utility towers) and clouds striking at certain points in the PV array whilst the other parts remain uniformly irradiated. Partial shading can dramatically reduce a PV panel's power and complicate the tracking process caused by multiple peaks in the P-V characteristic curve. Conventional MPPTs also find difficulties in tracking the global peak (GP) under

PSCs because they are not capable of differentiating between the local peak (LP) and the GP since *dP/dV* characteristics for both peaks are the same [40]. Therefore conventional MPPT algorithms usually fail to track the GP because it typically traps in a false power peak (local peak), as discussed in [40], [41]. The resulting output power significantly drops. Statistically, the output power could decrease by up to 30% [24], [42] of the total energy generated by PV systems.

Metaheuristic algorithms, such as PSO, are introduced for MPP tracking, particularly during PS. These algorithms successfully track the GP under PS with nearly zero oscillation at the MPP. However, the PSO or standard metaheuristic algorithm requires proper initialization and periodic tuning to ensure a good tracking performance. Improper initialization and parameter tuning result in unsatisfactory tracking performance. For example, large particles contribute to a long tracking time and convergence speed as the attribute reduces diversity or randomness in searching the optimal candidate, i.e., duty cycle [43]. As an alternative to standard metaheuristic, the idea of bioinspired optimization methods is mainly drawn from the intelligence of flocks, swarms, herds, or schools of creatures in nature. Such methods apply the behaviours of fireflies, bees, and birds in MPPT algorithms. In the literature, prominent bioinspired optimisation algorithms include CS [31], flower pollination algorithm [43], [44] ABC [32], grey wolf optimisation [45], firefly algorithm [46], fractional chaotic ensemble PSO [47], wind-driven optimisation [48], improved differential evolution (DE) [49], GA [50], cat swarm optimisation [51] and sliding mode control [52]. The disadvantages cited in [31], [43], [44], [51] are due to the high complexity of the searching mechanism that contributes to the computational burden relative to that of the proposed algorithm. In [36]–[39] the disadvantages include the high complexity of the structure, equation, and concept that contributes to the high initial oscillation and tracking time during the MPP tracking process compare with this proposed method. In [8], [32], [33], [43], [47], [51], the authors proposed an algorithm with a tracking time of more than 0.5 s and slow tracking relative to the proposed bio-inspired algorithm in the current work. The researchers in [35], [45]–[47], and [53] did not evaluate the proposed algorithm under dynamic changes in irradiance and the effectiveness of the developed algorithms was not clearly presented. The authors in [48], [49], [54]–[58] only performed tests under static conditions and did not analyze dynamic performance. In [52], the proposed MPPT technique was not evaluated under PSCs and was only tested under varying irradiance conditions.

The literature also presents a combination of conventional MPPT and soft computing MPPT, such as PSO blended with ANFIS [58], hybrid ABC with HC [59], Fuzzy blended with PSO [60], ACO blended with P&O [61], FPA with P&O [56], PSO with P&O [62] and PSO combined with DE to produce DEPSO [54], [63]. The results of these combinations show promising outcomes and implementation opportunities. However, mixing conventional and soft computing MPPT methods involve high complexity programming, implementation cost and computational burden in MPP tracking compare to simple concept and structure of proposed method in this paper.

Simple implementation, fast convergence speed, and accurate tracking are the main priorities for MPPT applications. Therefore, a new MPPT algorithm based on the salp swarm algorithm (SSA) is proposed in the current work. Seyedali Mirjalili introduced the SSA in [64]. It is one of the robust optimization algorithms among the bioinspired algorithms. The SSA is based on salp groups' swarming behaviour during ocean foraging and navigation. A swarm of salps remains connected, and a salp chain is never separated. The SSA has been proved to support exploitation by directing the search in every optimization problem towards an up-and-coming region in the search space around the right global optimum. This swarming behaviour is modelled, and the SSA is introduced to solve many optimization problems. In the current study, an improved application of the SSA–MPPT based on the direct duty cycle control strategy is presented to improve PV systems' efficiency. The SSA method comprises two simple steps involving mathematical functions: i) first salp (leader) equation and ii) direct control equation of followers to update the duty cycle/control variable with the first salp (leader) and second salp [3]. The proposed SSA method is compared and evaluated with several metaheuristics and a conventional algorithm (HC) to verify its viability. The proposed SSA, relative to the HC and other metaheuristic algorithms, can reduce high initial oscillation during the tracking process, thereby contributing to a low energy loss, improving tracking performance with a convergence speed of less than 500 ms, and facilitating the tracking of actual global optima with a reduced steady-state oscillation around the MPP [23]. A simple search mechanism in the proposed SSA exhibits good MPPT performance under dynamic irradiance changes, thus enhancing the amount of energy extracted from PV systems. The proposed SSA simulation results are validated with experimental work to prove the effectiveness and advantages of the method. Generally, the main contributions of this work are as follows:

- A simple novel bioinspired optimization method called the SSA is introduced to track the global maximum power point (GMPP).
- The proposed algorithm introduces a duty cycle boundary concept to direct the searching area towards the probable GMPP region. It has a straightforward control structure, simple implementation, low energy loss during the initial oscillation of the MPP tracking process, high convergence speed, and accurate tracking.
- The effectiveness of the proposed SSA is proved under various extreme environmental conditions.
- The proposed SSA is compared with the conventional HC and several other popular metaheuristics in terms of fast-tracking, convergence speed, and accurate tracking during sudden changes in irradiance conditions.

- The performance and effectiveness of the proposed SSA are validated based on simulation and experimental results.

The remaining parts of the article are: Section II describes the SSA as a new bioinspired optimizer. Section III discusses the application of the SSA to MPP tracking. Section IV discusses the advantages of SSA MPPT. Section V presents the simulation results and the comparison of the SSA with the conventional and metaheuristic methods. Section VI summarises the experimental validation. Section VII and VIII: limitation of proposed SSA and details the conclusion.

II. SALP SWARM ALGORITHM (SSA)

The body of salps and their movement are similar to those of jellyfish. Salps pump water through their tubular bodies as a driver to move forward. Salps are part of the *Salpidae* family and are characterized by transparent tubular bodies. Fig. 1 shows the shape of an individual salp. One of the most exciting characteristics of the SSA is behaviour swarming. The flock of salps illustrated in Fig. 2 is called the salp chain. The main factor for swarm behaviour is to use foraging and coordinated changes to find the best location for food sources.

FIGURE 1. Individual salp.

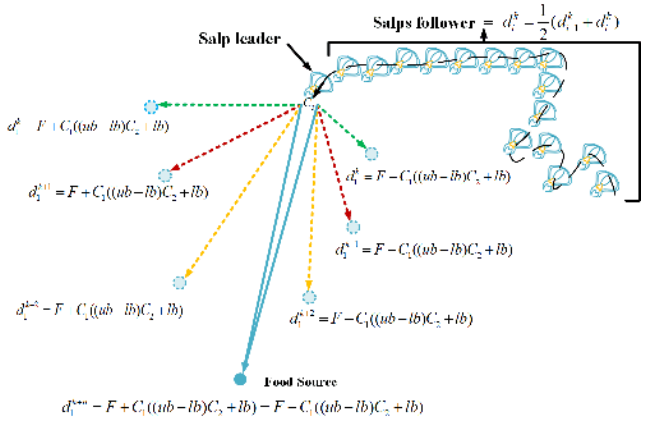

FIGURE 2. Swarm of salps (salp chain).

A. MATHEMATICAL MODEL

The goal of salp swarm behaviour is to locate food sources [31] by foraging and coordinating. The action can be modelled by mathematical functions to solve optimization issues. A salp swarm can be divided into leaders and followers. The salp leader is at the front of the salp chain whilst the rest of the salps in the chain are considered followers. The salp leader guides the swarm and is followed by the salp followers as they find food sources. The position of all salps in the swarm, their behaviour, and their populations are stored in a two-matrix array (row and column) called x. The target area of the salp swarm in the region of the matrix array is a food source called F. To update the salp leader's position, Seyedali Mirjalili [1] proposed the following equation:

$$x_1^k = F + C_1((ub - lb)C_2 + lb) \quad C_3 < 0.5 \tag{1}$$

$$x_1^k = F - C_1((ub - lb)C_2 + lb) \quad C_3 < 0.5 \tag{2}$$

where x_i^k is the position of the salp leader; F *is* the food source position; ub is the upper bound; lb is the lower bound; $i = 1$; and C_1, C_2, C_3 are random numbers. According to Equations (1) and (2), the salp leader's position is updated in accordance with the food source. Coefficient C_1 is a highly significant parameter for balancing exploitation and exploration in the SSA; it is defined as

$$C_1 = 2e^{-(\frac{4l}{L})^2} \tag{3}$$

where l and L are the current and maximum iterations, respectively. Parameters C_2 and C_3 are two random parameters with values between (0, 1) that are generated uniformly.

The following equations (Newton's law of motion) are used to update the position of the followers:

$$x_i^k = \frac{1}{2}at^2 + v_0 t \tag{4}$$

where $i \geq 2$, x_i^k is the ith position of the salp follower in the kth iteration, t is time, v_0 is the initial speed where $v = \frac{x - x_0}{t}$ and $a = \frac{v_{final}}{v_0}$. In the field of optimization, time is an iteration, the discrepancy between iterations is equal to 1, and $v_0 = 0$. This equation can be expressed as

$$x_i^k = \frac{1}{2}\left(x_{i-1}^k + x_i^k\right) \tag{5}$$

where $i \geq 2$ and x_i^k shows the position of the ith salp follower in the kth iteration. The swarm of salps is modelled using the mathematical model functions of Equations (1), (2), and (5).

B. ALGORITHM

The SSA creates a population of salp chains and begins to search for the global optimum by following a mathematical model of the salp chains (salp swarm). The salp leader in the SSA model initiates the search for a food source and directs the salp followers in the chain. When the food source is replaced with the global optimum, the salp swarm (salp chains) automatically moves towards it. The optimum food source is supposed to be chased by the salp leader responsible for guiding the salp followers to seek the food source. The best solution has yet to be obtained because of the unknown global optimum of optimization issues.

The SSA starts with the concept of finding the global optimum to initialize a randomly positioned swarm population of salps. It then evaluates each salp chain's fitness and searches for the salp with the desired fitness function optimization. It chooses the best fitting salp swarm position (variable F)

as the food source to be chased by the salp swarm [42]. The C_1 coefficient factor in Equation (3) is updated accordingly. Thereafter, the position of the salp leader is updated in Equations (1) and (2), and the salp followers are updated in Equation (5) for each iteration. Boundary conditions, i.e. upper boundary (*ub*) and lower boundary (*lb*) are set to prevent any salp from going outside the search area for optimization. The second step (evaluation of the fitness of each salp chain) is repeated until a criterion or end criterion is met.

The food source location is updated during the optimization of the salp chain in the search space via exploration and exploitation. The salp chain likely searches for and finds a good location and solutions. Fig. 3 shows that a moving food source can be found and chased by the modelled salp chain. With this movement and behaviour of the salp chain (a swarm of salps) towards the food source, it can move towards the global optimum which changes during each iteration. The coefficient C_1 is the single main SSA control parameter that drives the movement to explore the solutions through the search space and then exploit it.

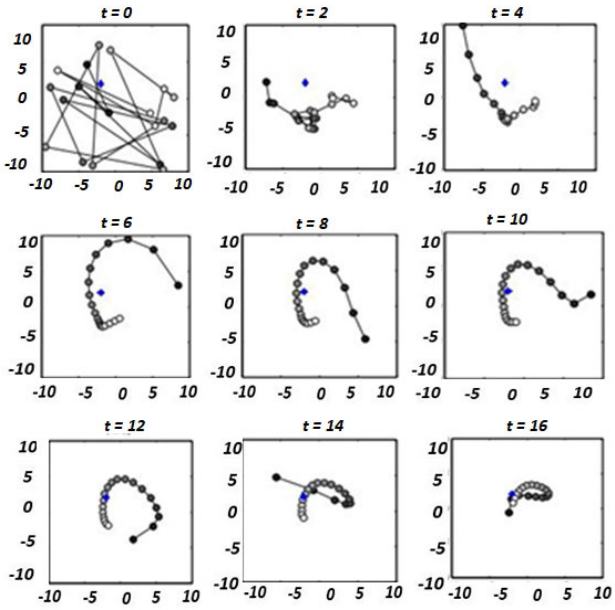

FIGURE 3. Salp chain movement around a stationary food source (Seyedali Mirjalili *et al.*, 2017).

III. MPPT TECHNIQUE USING SSA

Given the continuous variations in temperature and solar irradiance, the application of MPPT algorithms under dynamic environments is a primary concern. Under PSCs, an MPPT algorithm needs to deal with extreme changing environments. The standard SSA algorithm is only equipped to handle static optimization process. Direct employment of the algorithm will result in unsatisfactory tracking performance. The algorithm will not react to environmental changes once convergence to a single optimum is achieved. As a result, the operating point is maintained at a false operating point and a significant amount of power will be wasted. Even if the optimum shifts slightly in the event of a small change in irradiance, there is a continuous loss in power attainable from the PV system, which can significantly lower efficiency. To overcome this drawback, several improvements are proposed to the standard SSA to ensure dynamic tracking of the true optima and avoid severe losses. Fig. 4 shows the flowchart of the proposed SSA method for MPPT application. For simplicity of the algorithm, a direct duty cycle control strategy is utilized. Firstly, N_s salps determine the initial values of the duty cycles $x_i^k = d_i^k = [d_1, d_2, \ldots, d_i]$, $i = 1, 2, 3, \ldots, N_s$. Secondly, the algorithm reads and saves the tracked output power from the initial duty cycles sent to the DC-DC buck-boost converter. Thirdly, the algorithm evaluates the fitness function, i.e. the maximum output power set as an objective function. It then identifies the best fitness as the global best (*GBest*) position and updates the salp leader's position equation as follows: $d_1^k = GBest + C_1\left((ub - lb)\,C_2 + lb\right)$ and $d_1^k = GBest - C_1\left((ub - lb)\,C_2 + lb\right)$; base C_3 is a random probability switch ranging from 0 to 1 and then follows the Equation of the salp follower: $d_i^k = \frac{1}{2}\left(d_{i-1}^k + d_i^k\right)$. The C_1 coefficient is an important parameter defined in the SSA for balancing exploitation and exploration. $C_1 = 2\,e^{-\left(\frac{4\,l}{L}\right)^2}$, where L and l are respectively the maximum iterations and current iteration. C_2 is the random value generated uniformly in the interval [0, 1]. As a food source parameter, the F symbol is replaced with *GBest* (global best position) in the salp leader's position equation for MPPT application. Moreover, x is assumed to be equal to d, which denotes duty cycles. Finally, the MPP is identified, and the step is repeated

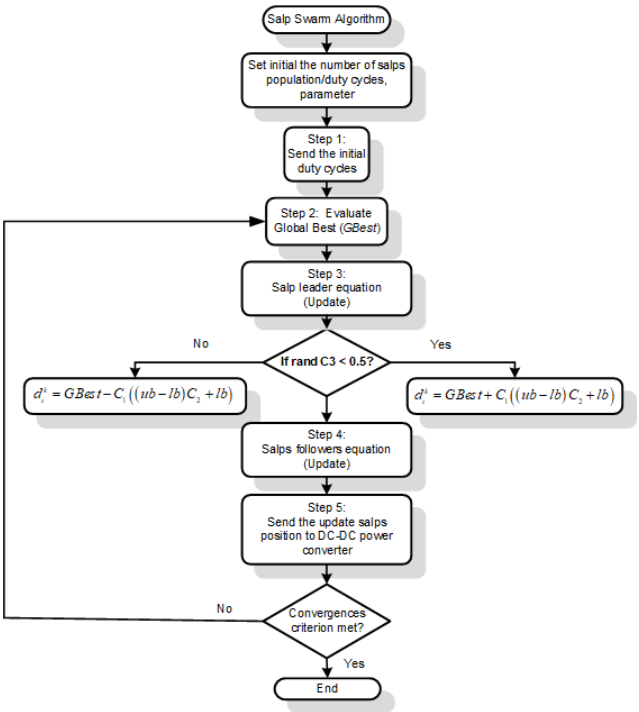

FIGURE 4. Flowchart of proposed SSA algorithm.

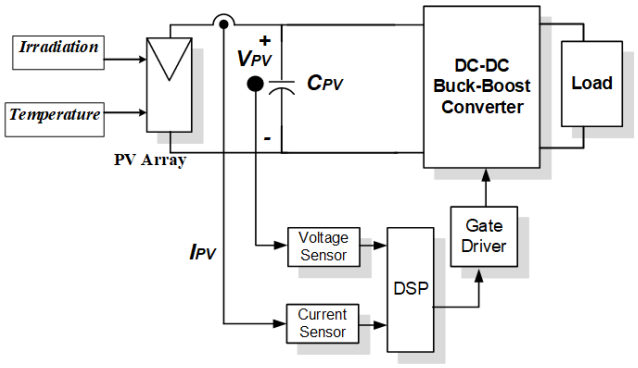

FIGURE 5. PV system with the DC-DC buck-boost converter.

until power convergence is achieved and the fitness value is satisfactory (Fig. 4).

The MPPT technique is mainly aimed at searching for a GMPP. Therefore, the objective function is defined as

$$P\left(d_i^{(k)}\right) > P\left(d_i^{(k-1)}\right)$$

where P is the power, k is the number of iterations and d is the duty cycle.

The nature of changes in dynamic environments highly influences the approaches that the algorithm can employ to recover from the changes. Therefore, the primary issue to be addressed is how to effectively detect the changes and differentiate the severity of changes in the P-V landscape. Changes in the environment can cause the P-V landscapes in the MPPT problem to vary from a single peak to a single peak (uniform to uniform irradiance conditions), a single peak to multiple peaks (uniform irradiance to PS conditions), and multiple peaks to multiple peaks (PS to PS conditions) at different rates of frequency changes. To enable standard SSA algorithm to deal with dynamic MPPT problem effectively, the following re-initialization shown in Equation (6) is used to reset the positions of the salps:

$$\left|\frac{P_i^{(k)} - P_i^{(k-1)}}{P_i^{(k-1)}}\right| > \Delta P \tag{6}$$

$$\eta = \frac{\text{Tracked Power } (\text{P}_{Tracked})}{\text{Actual PV Power } (Output)} \times 100\% \tag{7}$$

IV. ADVANTAGES OF THE PROPOSED SSA

For fast and accurate tracking performance, the initial duty cycles need to explore a wide P-V curve area. Thus, the number of initial duty cycle (D) is an essential and critical aspect that needs to be carefully considered in determining the effectiveness of the tracking process. A large (D) improves the search efficiency (i.e., probability of tracking to the correct value) but contributes to long convergence and tracking time. In the proposed SSA-MPPT, comprehensive simulations indicate that $D = 3$ is a reasonable compromise and is therefore used in this study.

Another modification that has been proposed is a determination of the correct boundary limit to ensure effective tracking. In this work, a parameter called duty cycle boundary (DCB) is introduced. It is defined as the upper and lower boundary of the duty cycle (D_U, D_L). By limiting the duty cycle value within the DCB, the maximum explorable area during the optimization process is reduced. The determination of DCB is done based on the concept of voltage-current range (VCR). VCR is the range in which the MPP could be located. For clarity, the proposed SSA's searching mechanism during uniform irradiation is shown in Fig. 6. Only one sample is used to represent the movement of duty cycle (D) to demonstrate the advantages of the proposed SSA and how the modifications made contribute to the fast-tracking and high convergence speed. The upper subscription of the variable duty cycle in Fig. 7 shows the number of tracking iterations. In the first iteration, the proposed SSA tracks the global best position (GBest). Subsequently, it moves towards (Gbest) in the same direction. To update the new direction and position of salp based on the salp leaders, Equations (1) and (2) are used. It is then followed by the salp follower in Equation (5). By implementing the direct GBest technique in the proposed method, particle salp movement moves straight forwards to the potential target with a skipped region for searching. Compared to the PSO algorithm, it only uses GBest and personal Best (PBest) to update the new velocity. This is a crucial

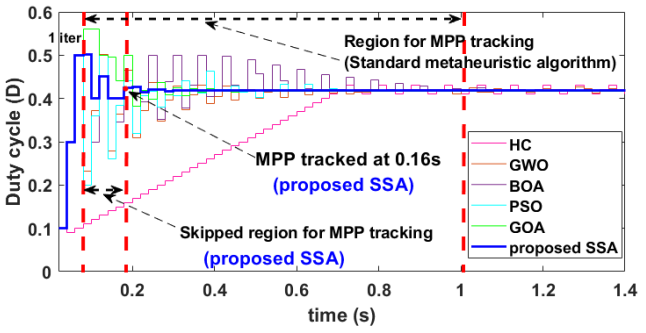

FIGURE 6. Advantages of proposed SSA in MPP searching mechanism for the PV systems.

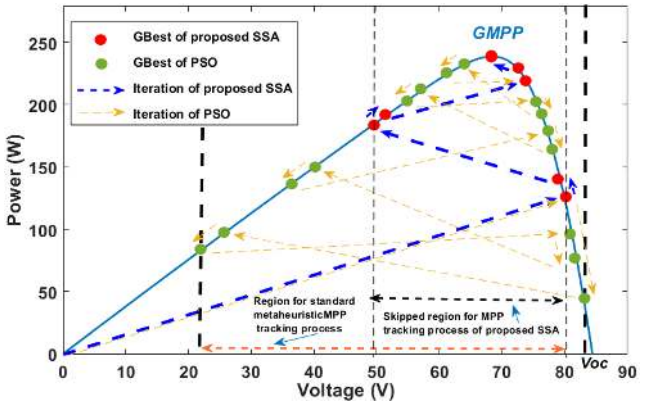

FIGURE 7. Duty cycle illustration during the tracking process.

parameter to generate the new direction for each particle swarm and is often employed in other standard metaheuristic algorithms. This step contributes to long tracking time, slow convergence speed, and high initial oscillation during the tracking process. Consequently, a large amount of energy will be wasted. Based on the illustration of the duty cycle in Fig. 7, the proposed SSA algorithm only requires four iterations to find GMPP. Moreover, only C_1 coefficient plays a vital role in balancing the exploitation and exploration capabilities.

As shown in Fig. 7, the PSO algorithm's duty cycle requires 10 iterations to find the GMPP based on the PSO principle discussed in [30], [65]. Fig. 6 and Fig. 7 systematically show the advantages of the proposed method to skip unnecessary regions during GMPP tracking process, hence improving its effectiveness. The PSO algorithm [30] and other metaheuristic algorithms with a similar structure will contribute to long tracking time, slow convergence speed, and steady-state error around MPP. Fig. 6 clearly shows that the proposed SSA outperforms the other metaheuristic algorithms and conventional HC algorithm in terms of fast-tracking, high convergence speed, reduced high initial exploration process, and zero steady-state oscillations around MPP.

V. SIMULATIONS RESULTS

The proposed SSA–MPPT algorithm is simulated and analyzed using a MATLAB/Simulink platform. Fig. 5 shows the overall simulation block diagram of the PV system which includes a buck-boost converter and an MPPT controller. The following parameter specifications of the converter: $L = 1$ mH, $C_1 = 470$ μF, $C_2 = 220$ μF, and $f = 20$ kHz. In this work, the PV array is made up of four series-connected PV modules. As the MPPT sampling time is crucial because MPP readings should be taken upon reaching a steady-state condition, the sampling time of the SSA–MPPT controller is set to 0.02 s. Simulations are carried out with large step changes in the uniform irradiance condition (Fig. 9), followed by large step changes in PSCs, as shown in Figs. 13 and 14.

A. SIMULATION WITH LARGE STEP CHANGES IN UNIFORM IRRADIANCE CONDITIONS

The performances of the HC, GWO, BOA PSO, GOA, and SSA based on MPPT during large step changes in uniform irradiance conditions are evaluated in terms of fast-tracking capability, oscillation in duty cycles, and convergence speed. For large step changes, the irradiance is initially set to 1,000 W/m^2 at time $t = 0$ (point 1), reduced to 500 W/m^2 at $t = 2$ s (point 2) and finally increased to 800 W/m^2 at $t = 4$ s (point 3) (Fig. 8). The temperature is set to be constant at 25 °C. The tracking responses of the HC, GWO, BOA, PSO, GOA and SSA–MPPT are presented in Fig. 9.

The SSA starts its optimization process by initially sending three random duty cycles and then updates the salp leader's equation to find the GMPP based on a random number C_3. Finally, it proceeds with the follower equation for the rest of the salps. The coefficient C_1 parameter is based on Equation (3), which governs the balance between

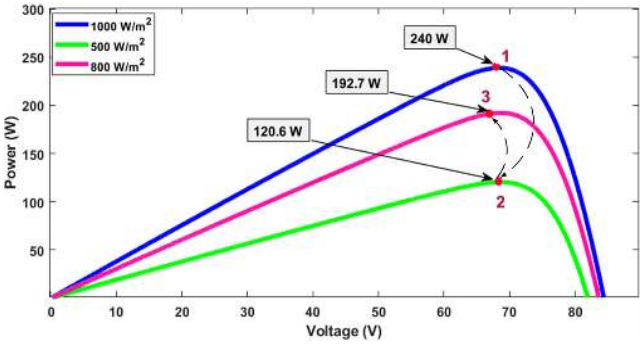

FIGURE 8. *P-V* curves during uniform solar irradiance.

exploitation and exploration of the SSA. As shown in Fig. 9-(SSA), particularly for the large step change response from 0 s to 2 s, C_1 governs the SSA in tracking and converging at the real GMPP (239.6 W) within 0.16 s; such speed is faster than that of GOA (GMPP = 239.3 W) in 0.48 s (Fig. 9-(GOA)), PSO (GMPP = 239.1 W) in 0.6 s (Fig. 9-(PSO)), BOA (GMPP = 239.1 W) in 0.83 s (Fig. 9-(BOA)), GWO (GMPP = 239.3 W) in 0.71 s (Fig. 9-(GWO)). In contrast, HC only tracks (GMPP = 237 W) within 1 s, representing the slowest response for the conventional algorithm. Within 2–4 s (i.e. 2.16 s), the SSA can converge and track the maximum point (Fig. 9-(SSA)) and is thus faster than other metaheuristic algorithms: GOA, PSO, BOA, GWO, and HC, the convergence speeds are 2.3 s (Fig. 9-(GOA)), 2.5 s (Fig. 9-(PSO)), 3.3 s (Fig. 9-(BOA)), 2.71 s (Fig. 9-(GWO)) and 2.3 s (Fig. 9-(HC)), respectively. Within 4–6 s, the SSA converges and tracks the GMPP (192.6 W) in 4.19 s (Fig. 9-(SSA)) and is thus faster than the GOA, which tracks the GMPP (192.2 W) in 4.6 s (Fig. 9-(GOA)), PSO which tracks the GMPP (192.1 W) in 4.6 s (Fig. 9-(PSO)), BOA which tracks the GMPP (192.1 W) in 4.56 s (Fig. 9-(BOA)), GWO which tracks the GMPP (192.2 W) in 4.73 s (Fig. 9-(GWO)) and HC, which tracks the GMPP (191.4 W) within 4.2 s (Fig. 9-(HC)). The results presented in Fig. 9 further indicates that the GOA–, PSO–, BOA–, GWO–MPPT algorithm can reach the MPP but with high oscillation during the initial exploration process. Fig. 10, Fig.11, and Fig.12 show the average maximum output power tracked and the maximum number of iterations for each method in 100 runs under uniform conditions. In conclusion, the proposed SSA–MPPT algorithm (Fig. 9-(SSA)) has a relatively low oscillation during the initial exploration. The conventional HC–MPPT algorithm produces high steady-state oscillation near the MPP (Fig. 9-(HC)) during step-down and step-up conditions with sluggish tracking performance.

B. SIMULATION WITH LARGE STEP CHANGES IN PSC

The capabilities and performances of the HC, GWO, BOA, PSO, GOA, and SSA based MPPT are further validated with large step changes in PSCs. Their performances are compared in terms of their tracking speed and oscillation during the

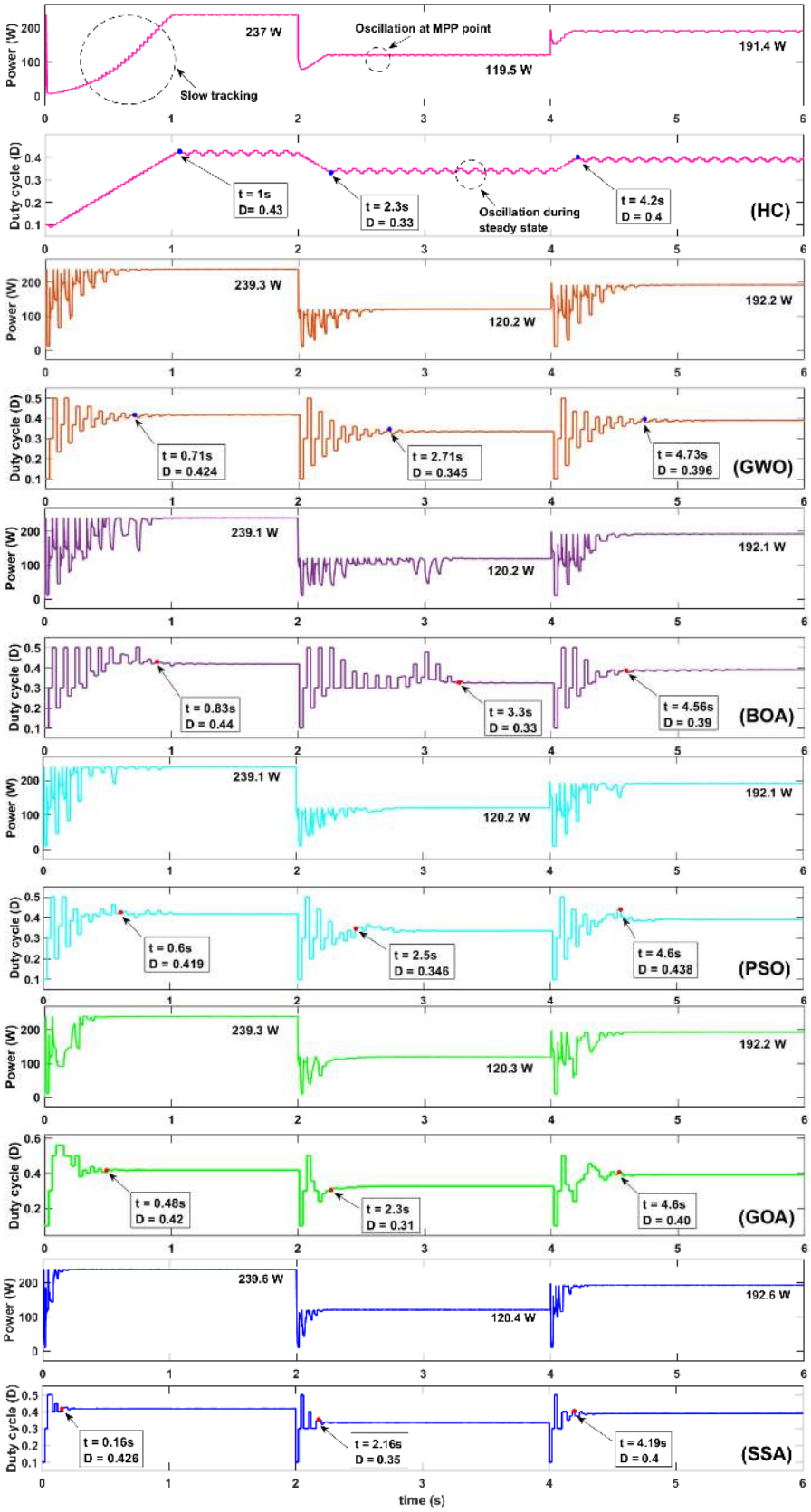

FIGURE 9. Tracking responses of SSA, GOA, PSO, BOA, GWO, and HC during large step changes in uniform irradiance.

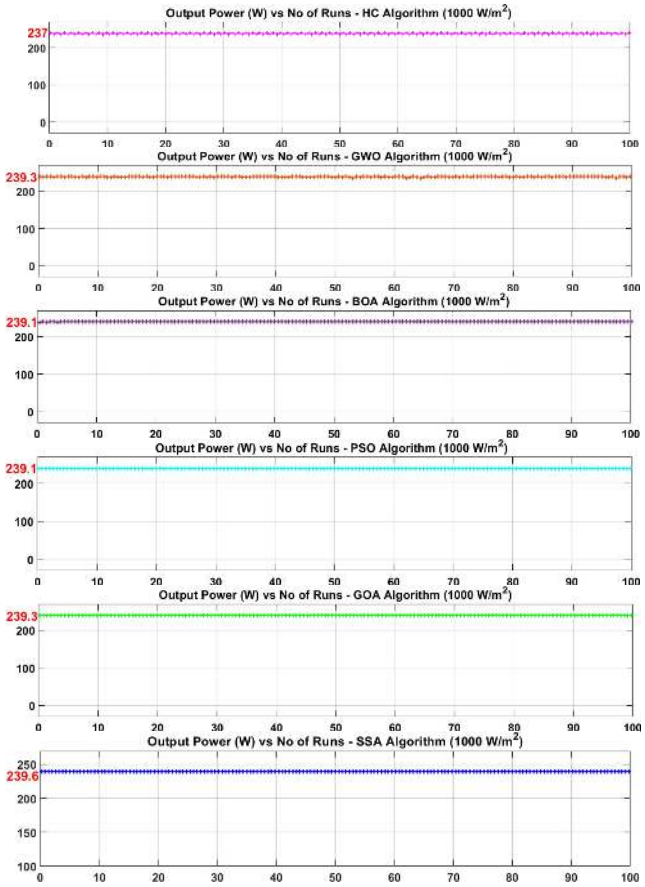

FIGURE 10. Convergence characteristics of output power for 100 runs (1000 W/m^2).

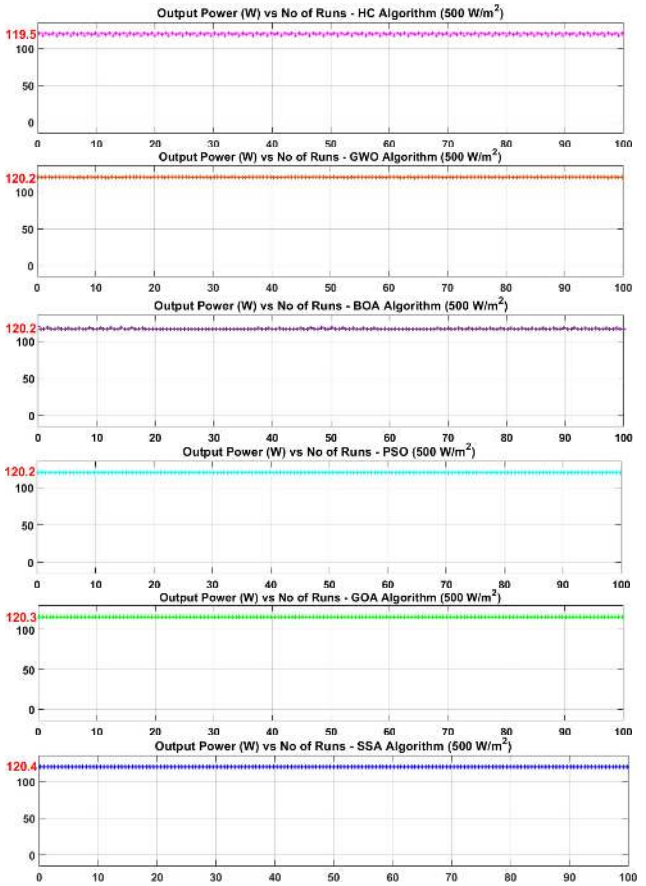

FIGURE 11. Convergence characteristics of output power for 100 runs (500 W/m^2).

tracking process. Their abilities to track the true MPP for three different patterns are also compared. Figs. 13 and 14, respectively show the configurations and *P-V* curves of the three different patterns. Pattern (A) produces two peaks with GP at 177 W. Pattern (B) produces three peaks with GP at 136.5 W, and pattern (C) produces two LPs with GP at 114.5 W. As for the evaluation of the large step changes in the three different pattern conditions, the test initially starts with pattern (B) (point 1) at time $t = 0$ and then shifts to the pattern (C) (point 2) at $t = 2$ s. In the last evaluation, it changes to the pattern (A) at $t = 4$ s. Fig. 15 shows the simulation results of the evaluated MPPT controllers.

The simulation results of the HC, GWO, BOA, PSO, GOA, and SSA based MPPT during large step changes in PSC from 0 s to 2 s (see Fig. 15-(SSA), pattern B) are evaluated. The SSA based MPPT approaches the GMPP (136.3 W) in 0.22 s. During this condition, C_1 governs the SSA to converge the duty cycle at 0.41 to reach the GMPP within 0.22 s. Hence, the proposed algorithm is superior in terms of convergence speed, which is 0.51 s faster than GOA, which reaches the GMPP of 136.2 W, 0.7 s more quickly than PSO that reaches the GMPP (136.1 W), 0.83 s faster than BOA that reaches the GMPP of 135.1 W and 0.89 s faster than GWO that reaches the GMPP at 136 W. The GOA–, PSO–, BOA–, GWO–MPPT algorithm shows high initial exploration process oscillation as shown in Fig. 15-(GOA), Fig. 15-(PSO), Fig. 15-(BOA), Fig. 15-(GWO). For HC, the algorithm is trapped at the local MPP (110.3 W, see Fig. 15-(HC)).

At $t = 2$ s, the PS pattern changes from pattern B to pattern C and remains the same for around 2 s. The SSA detects a change in power that satisfies the re-initialization condition and accordingly reacts to swiftly reach a new GMPP (114.3 W) within 2.3 s. Relative to SSA, the GOA–, PSO–, BOA– reaches the GMPP (113.9 W) in 2.4 s (Fig. 15-(GOA)), GMPP (114 W) in 2.9 s (Fig. 15-(PSO)), GMPP (112.6 W) in 3.1 s (Fig. 15-(BOA)) and GWO–MPPT trapped in local MPP (95.56 W) with steady-state oscillation at MPP point (Fig. 15-(GWO)). An apparent oscillation can also be observed during the tracking process (2 s – 4 s), as shown in Fig. 15 for GOA–, PSO–, BOA–, GWO–MPPT. For HC, it is trapped again at the local MPP (55.01 W) at 2.3 s (Fig. 15(HC)).

At $t = 4$ s, another change in PSC occurs. The PS pattern shifts from pattern C to pattern A. The SSA successfully tracks the GMPP (176.9 W) in 4.2 s (Fig. 15-(SSA)). The convergence speed for reaching the GMPP is around 0.2 s, which is 0.42 s faster than that of the GOA algorithm. GOA successfully tracks the GMPP (176.5 W) in 4.62 s (Fig. 15-(GOA)). The SSA is 0.5 s faster than that of the PSO algorithm. PSO successfully tracks the GMPP (176.5 W)

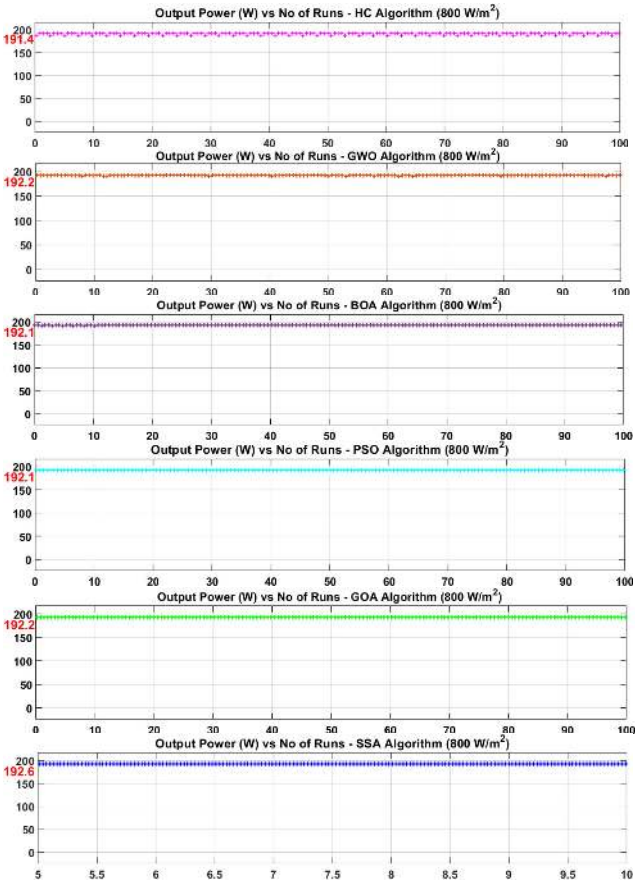

FIGURE 12. Convergence characteristics of output power for 100 runs (800 W/m^2).

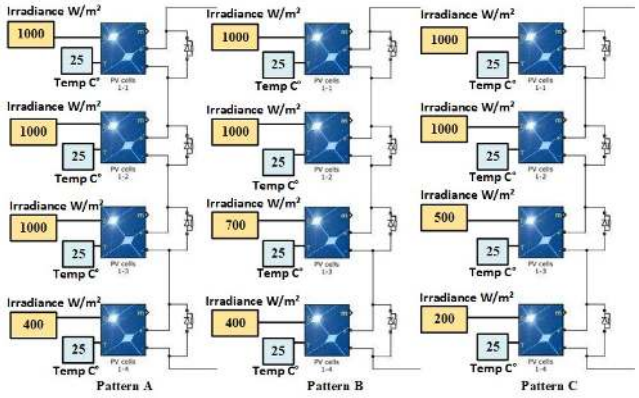

FIGURE 13. PV array configurations of tested patterns.

in 4.7 s (Fig. 15-(PSO)). BOA and GWO successfully track the GMPP (176.4 W) in 4.56 s (Fig. 15-(BOA)) and the GMPP (176.4 W) in 4.84 s (Fig. 15-(GWO)). The convergence of SSA is 0.36 s and 0.64 s faster than BOA and GWO, respectively. The HC algorithm trapped at the local MPP (111.3 W). As shown in Fig. 15-(HC), high steady-state oscillation is apparent near the MPP. The average maximum output power tracked versus the maximum number of

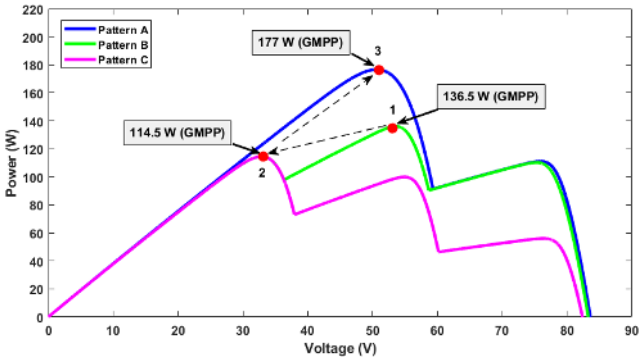

FIGURE 14. *P-V* curves of different partial shading patterns.

iterations for each method in 100 runs under PSCs are shown in Fig. 16, Fig. 17, and Fig. 18.

According to the simulation results of (1) large step changes in uniform irradiance conditions and (2) large step changes in PSCs, the SSA achieves exceptional tracking performance in terms of tracking accuracy, convergence speed, and oscillation around the MPP. It outperforms GOA, PSO, BOA, GWO, and HC in all tested criteria. Table 1 summarises the tracking performances of SSA, PSO, GOA, GWO, BOA, and HC under the tested conditions. The SSA achieves the highest average tracking efficiency under uniform conditions of 99.87%, followed by PSO, GOA, GWO, BOA, and HC with 99.66%, 99.73%, 99.70%, 99.66%, and 99.06%, respectively. For the large step changes in PSC, the average MPP tracking efficiency of SSA is 99.87% followed by PSO, GOA, GWO, BOA, and HC with 99.66%, 99.65%, 94.25%, 98.99%, and 63.91%, respectively.

The qualitative comparison in terms of periodic tuning, tracking speed, convergence speed, sensed parameter, steady-state oscillation, dynamic response, tracking accuracy, and initial MPP tracking process are presented in Table 2. The efficiency for MPPT is estimated by the trade-off between LMPP and GMPP. A proper trade-off between these two search processes can lead to a precise approximation of GMPP position. If the optimization process focuses closely on the local search process, then the MPPT achieves a high converge speed but is likely to become trapped at the local optima. Minimizing this probability calls for a large exploration search coefficient, C_1, for a global mode search. In the proposed SSA, only one salp leader is utilized to balance the local and global MPP search. By controlling the coefficient, C_1, the global MPP search coefficient gradually decreases as the number of optimization iterations increases.

Relative to all metaheuristic algorithms and conventional algorithms in Table 1 and Table 2, the proposed SSA can easily track the real MPP in any environmental circumstance by using a small particle population and exploiting the advantages of bioinspired group behaviour. Another critical aspect of dealing with the MPPT problem is the algorithm's ability to deal with dynamic environments. The initially formed population of the SSA is dispersed randomly in the search space.

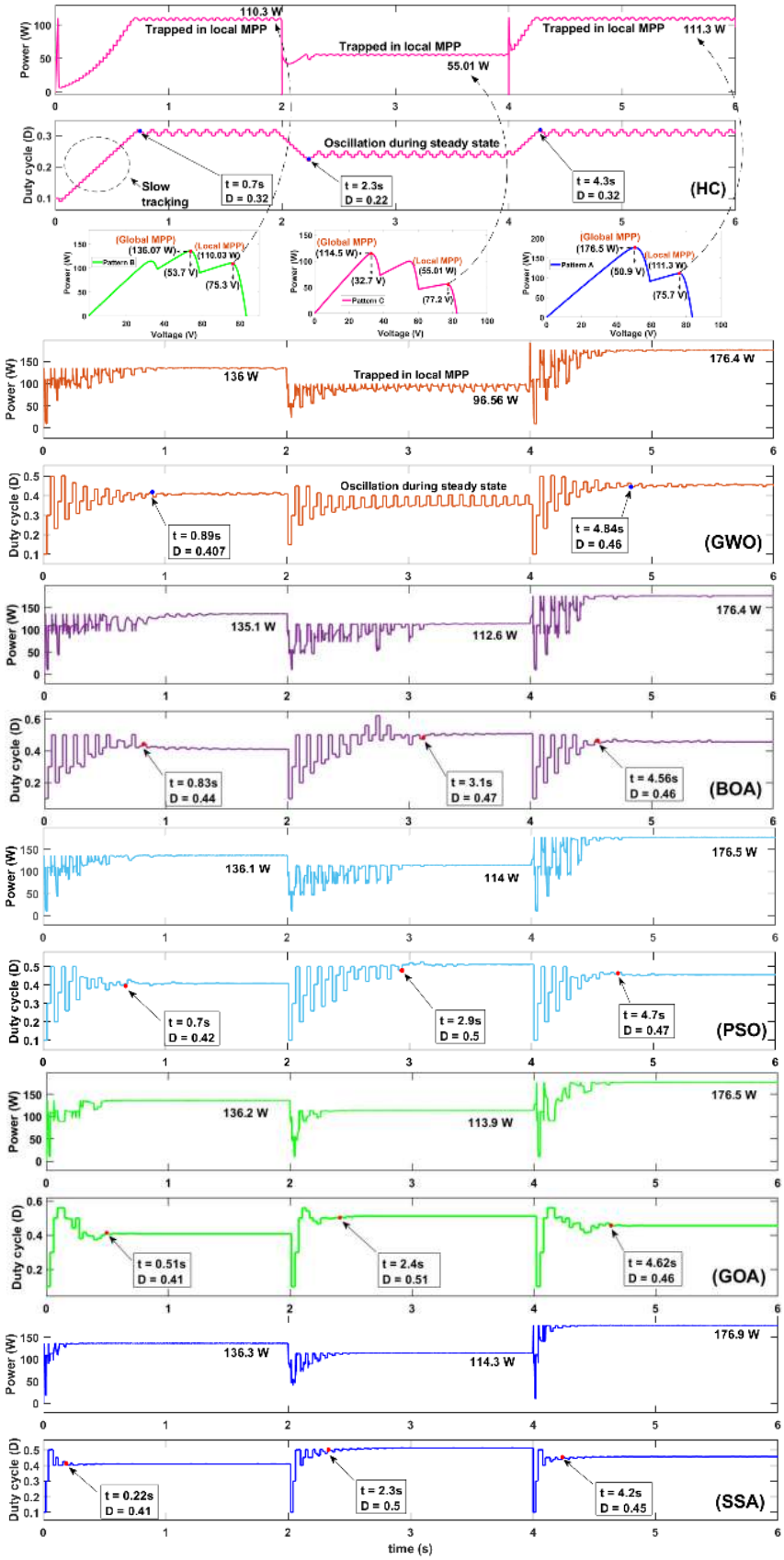

FIGURE 15. Tracking responses of SSA, GOA, PSO, BOA, GWO and HC during large step changes in PSC.

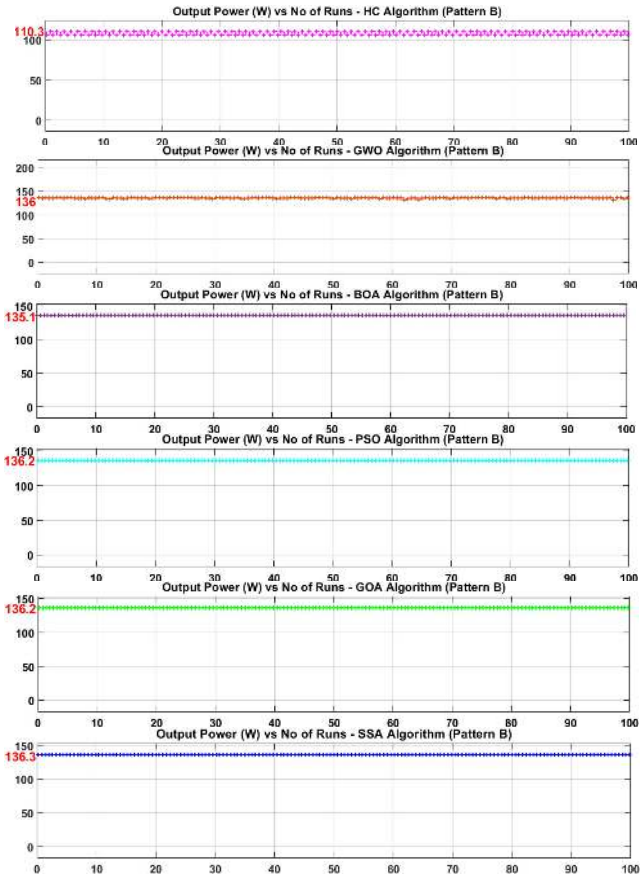

FIGURE 16. Convergence characteristics of output power for 100 runs (Pattern B).

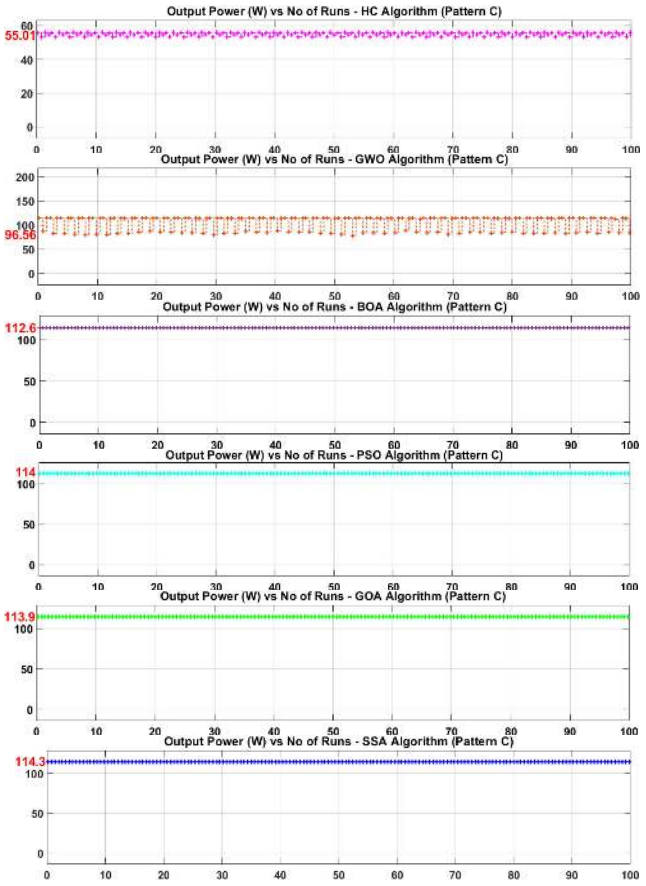

FIGURE 17. Convergence characteristics of output power for 100 runs (Pattern C).

This feature enables the algorithm to explore in a larger area. The SSA converges to an optimal solution with all particles and leads to loss of diversity. However, the loss of diversity is not tricky in static locations. While it is not acceptable in a dynamic MPPT condition. It is necessary to identify the GMPP whenever changes occur in atmospheric conditions. To overcome this issue, the proposed SSA refreshes the information via re-initialization to adapt to dynamic environments. With the proposed modifications, the proposed SSA is envisioned to become one of the superior choices of MPPT algorithms.

VI. EXPERIMENTAL VALIDATION

An experimental setup shown in Fig. 19 is developed to validate the performance of the proposed SSA–MPPT algorithm. The commercial PV array simulator by Chroma ATE Inc. (Model: 62050H-600S) is employed to emulate the PV arrays' real characteristics. The PV simulator is connected to a load via the 500 W DC-DC buck-boost converter. Its component specifications are similar to the parameter specifications used in simulations. MOSFET and fast recovery diode are utilized for power switching devices. The proposed MPPT technique is implemented on the Texas Instruments TMS320F28335 DSP controller. The programming is developed in a MATLAB/Simulink® embedded coder platform integrated with Code Composer Studio (CCS) for a rapid software development process. Similar to the simulation setup, four series-connected PV modules (MSX-60 by SOLAREX) are considered for the experimental work. The PV array (MSX-60) has the following specifications: maximum power (P_{max}) = 59.85 W, voltage at MPP (V_{mpp}) = 17.1 V, current at MPP (I_{mpp}) = 3.5 A, short circuit current (I_{sc}) = 3.8A and open-circuit voltage (V_{oc}) = 21.8 V.

The proposed MPPT algorithm is tested under four different scenarios: (1) under uniform irradiance, (2) under static PS, (3) under step change between uniform irradiances, and (4) under transitions between uniform irradiance and PSCs. The maximum PV output power for 4 × 1 array at standard test conditions (STC) is 240W.

For uniform test conditions, the level of irradiance starts at 1000W/m^2. It is then followed by a step-change in irradiance where the irradiance level drops to 500W/m^2. Finally, the level of irradiance increases back to 800W/m^2. Fig. 20 shows the waveforms of power, current, and voltage during the MPP tracking process. The MPP tracking point with a red dot represents the exact operating point of the system on *I-V* and *P-V* curves. In the first condition, when irradiance is at 1000W/m^2, the real output power is 239.3 W. As can be seen in Fig. 20 (a), the proposed algorithm successfully

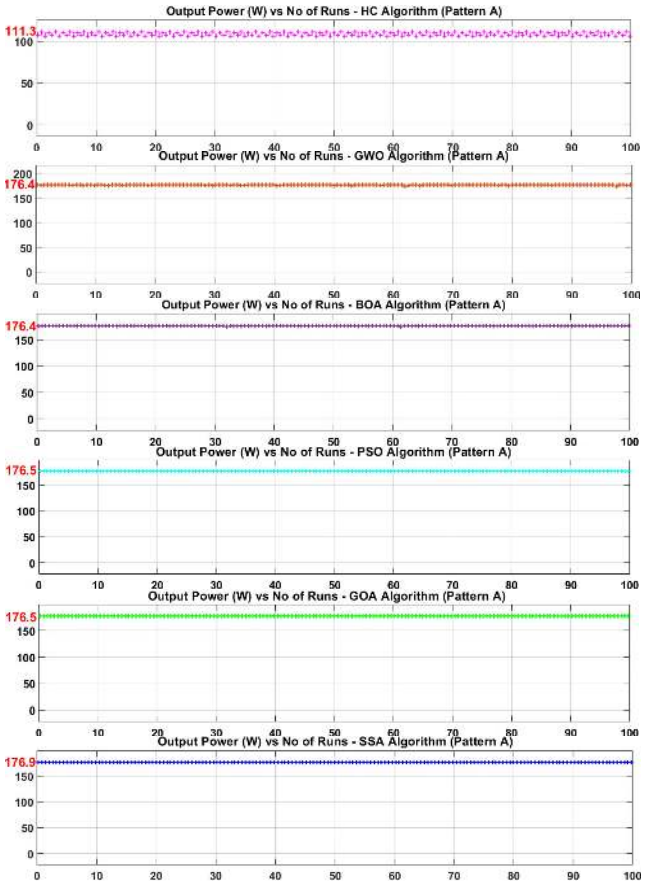

FIGURE 18. Convergence characteristics of output power for 100 runs (Pattern A).

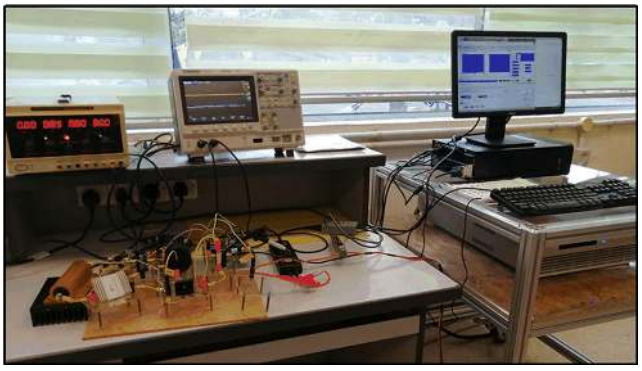

FIGURE 19. Laboratory prototype of the proposed MPPT system.

tracks the MPP at 239.1 W. The MPP tracking efficiency of 99.95% is achieved. For the transition from condition 1 (1000W/m^2) to condition 2 (500W/m^2), the accuracy of salp during MPP exploration is clearly demonstrated. It tracked power is 120.1 W, where the PV array model output power is 120.3 W. Thus, the tracking efficiency of 99.9% is achieved as shown in Fig. 20(b). Fig. 20 (c) shows the transition between condition 2 to condition 3. Again, high accuracy, fast-tracking ability, and high convergence speed are proven. The MPP is successfully tracked with 99.95% efficiency, as can be seen in Fig. 20 (c).

Fig. 21 shows the waveform of PV power, current, and voltage for experimental validation of the proposed method under step change in PSCs. For PSC-Pattern B (condition 1), as shown in Fig. 21, the GMPP is tracked at 136.0 W, in which the PV array model output power is 136.1 W. The MPP tracking efficiency reached up to 99.96%, with low steady-state oscillation around MPP as displayed in Fig. 21(a). For the second condition (transition from pattern B to pattern C), the proposed method successfully tracked the GMPP at 113.6 W. The MPP tracking efficiency is 99.21%. Finally, the last transition is from PSC-Pattern C to PSC-Pattern A. The tracking efficiency is maintained at around 99%, in which the tracked power is 175.7 W. For all three conditions tested, the tracking response of the proposed method exhibit excellent performance. The tracking accuracy achieved more than 99% for all conditions tested with fast-tracking and convergence speed.

For the third test, the proposed SSA's performance is validated for a transition from uniform condition (1000W/m^2) to PSC-Pattern C. The tracking response of voltage, current, and power is shown in Fig. 22. The tracked power at 1000W/m^2 is 239.2 W, which corresponds to 99.96% efficiency. As soon as the partial shading conditions occur (PSC-Pattern C), the algorithm detects the significant variation in array power. The algorithm again sends the initial particles to the converter. Fluctuations in the operating point can be seen during the exploration stage. This is due to the multimodal *P-V* landscape as illustrated in Fig. 22 (b). The new global MPP is achieved in the third population and the array power, voltage, and current are valued at 114 W, 32.6 V, and 3.5 A, respectively. Until the next change is able to satisfy the threshold value in equation (6), the algorithm continues to operate at this operating point.

Further tests are performed for 4 $\times$ 1 array with a maximum output power of 60 W at STC. Firstly, evaluation under a static uniform condition test is done. The PV array is set to 800W/m^2 irradiance (Fig. 23). The tracking response is shown in Fig. 24. The proposed SSA method accurately tracks the GMPP (48.07 W). Moreover, the SSA tracks the MPP in less than 500 ms with an efficiency of 99.92%. Under PSC, the proposed SSA is verified for pattern 1 (Fig. 25) (where the modules' irradiances are 1,000, 800, 500, and 300 W/m^2, respectively). Fig. 25 shows the *I-V* and *P-V* curves for the PS test of condition 1. The tracking response in Fig. 26 indicates that the proposed SSA successfully and accurately finds the true GMPP (23.03 W) under PSC. The tracking speed is less than 1.5 s, and the MPPT efficiency is 99.96% based on Equation (7).

The next experiment is conducted to assess the proposed SSA performance during a step change in irradiance under uniform irradiance conditions. During this test, the irradiance remains at 800 W/m^2 for 6 s and then falls to 700 W/m^2. Figs. 23 and 27 illustrate the *I-V* and *P-V* curves for both conditions. The MPP tracking result in Fig. 28 shows that

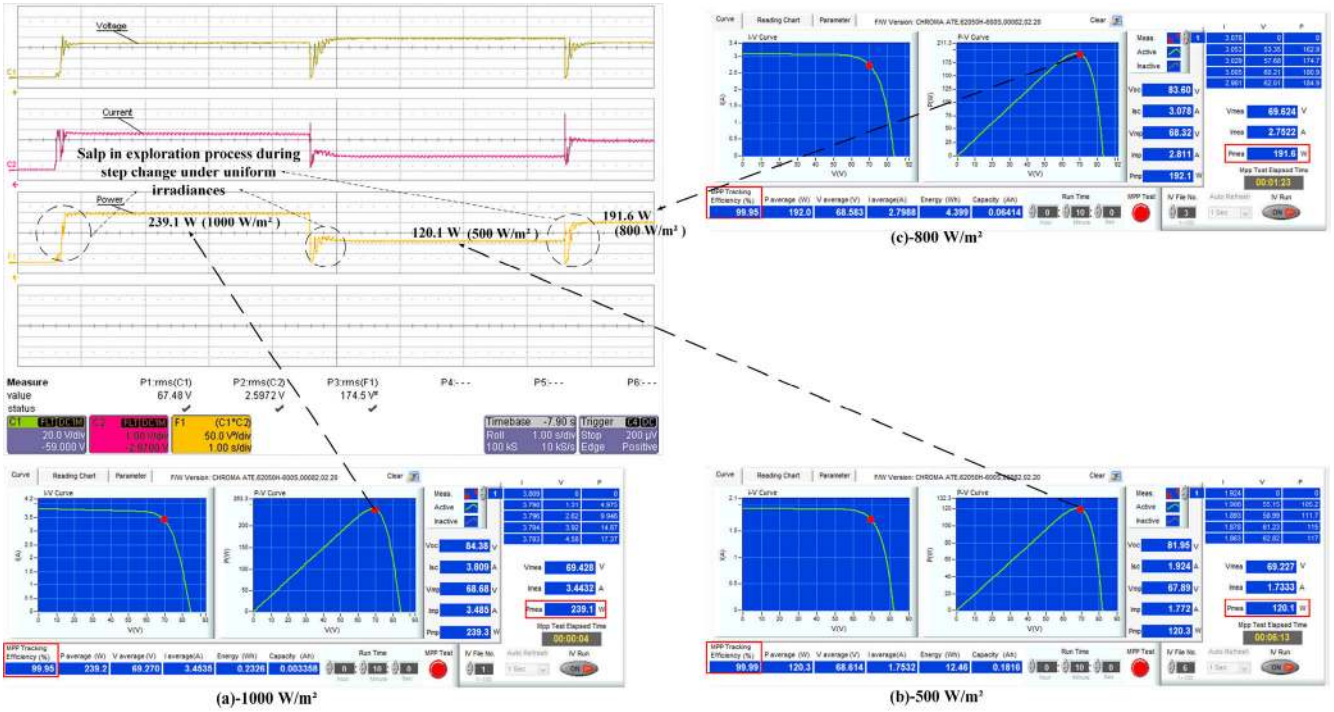

FIGURE 20. *I-V* and *P-V* curves under step change for uniform conditions.

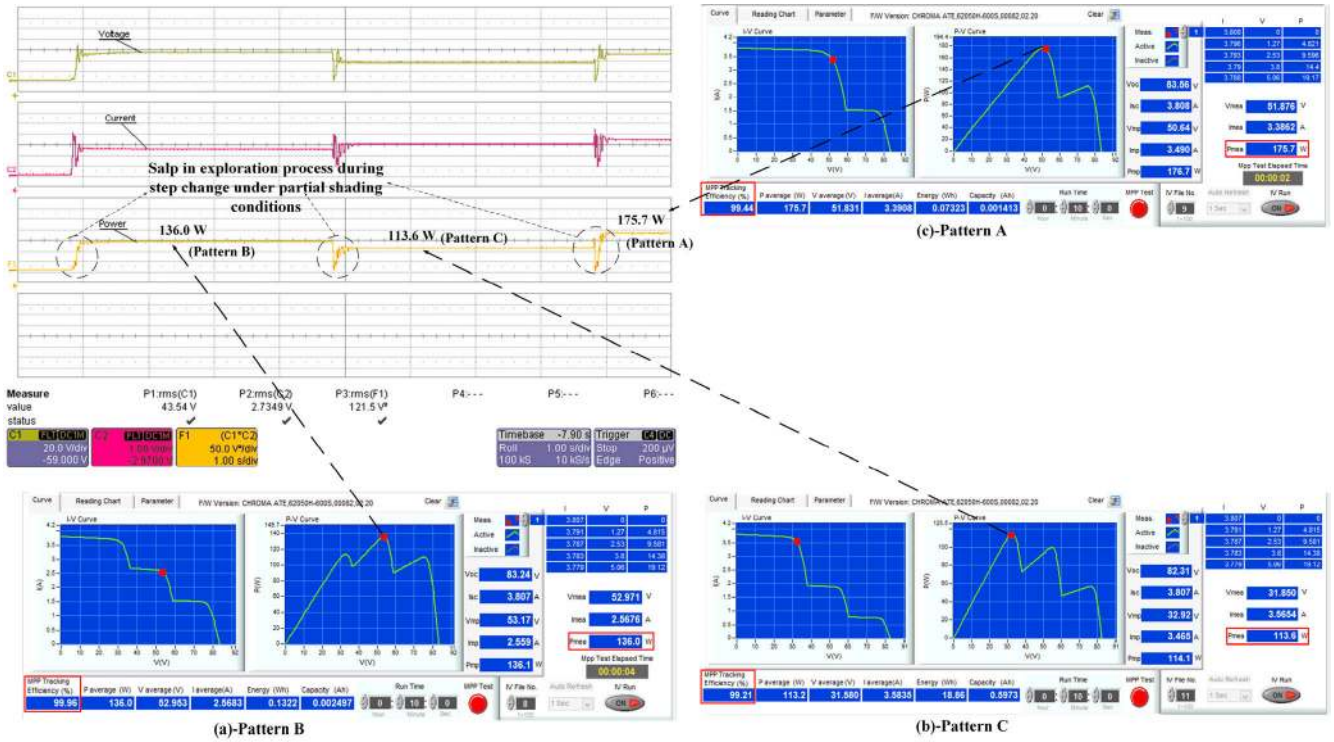

FIGURE 21. *I-V* and *P-V* curves under step change for PSCs.

the proposed SSA successfully finds the GMPP (48.07 W) within 0.3 s under a uniform condition at 800 W/m^2. At the transition from 800 W/m^2 to 700 W/m^2, the proposed SSA swiftly reacts to the dynamic change in the environment (step change in irradiance) and successfully reaches the GMPP (42.18 W). The tracking time to reach the new

TABLE 1. Tracking efficiencies of proposed SSA, conventional and metaheuristic method under large step changes.

Step large changes response (time)	PV array model output	Power *MPP, (W)* (P_{MPP})						Efficiency, η MPPT					
(A)Under Uniform conditions		SSA	PSO	GOA	GWO	BOA	HC	SSA	PSO	GOA	GWO	BOA	HC
0-2s	240	239.6	239.1	239.3	239.3	239.1	237	99.83%	99.63%	99.70%	99.70%	99.63%	98.75%
2-4s	120.6	120.4	120.2	120.3	120.2	120.2	119.5	99.83%	99.67%	99.75%	99.67%	99.67%	99.09%
4-6s	192.7	192.6	192.1	192.2	192.2	192.1	191.4	99.95%	99.69%	99.74%	99.74%	99.69%	99.33%
Average Efficiency, η MPPT								99.87%	99.66%	99.73%	99.70%	99.66%	99.06%
(B)Under partial shading conditions		SSA	PSO	GOA	GWO	BOA	HC	SSA	PSO	GOA	GWO	BOA	HC
0-2s	136.5	136.3	136.1	136.2	136	135.1	110.3	99.85%	99.71%	99.78%	99.63%	98.97%	80.81%
2-4s	114.5	114.3	114	113.9	95.56	112.6	55.01	99.83%	99.56%	99.47%	83.46%	98.34%	48.04%
4-6s	177	176.9	176.5	176.5	176.4	176.4	111.3	99.94%	99.71%	99.71%	99.66%	99.66%	62.88%
Average Efficiency, η MPPT								99.87%	99.66%	99.65%	94.25%	98.99%	63.91%

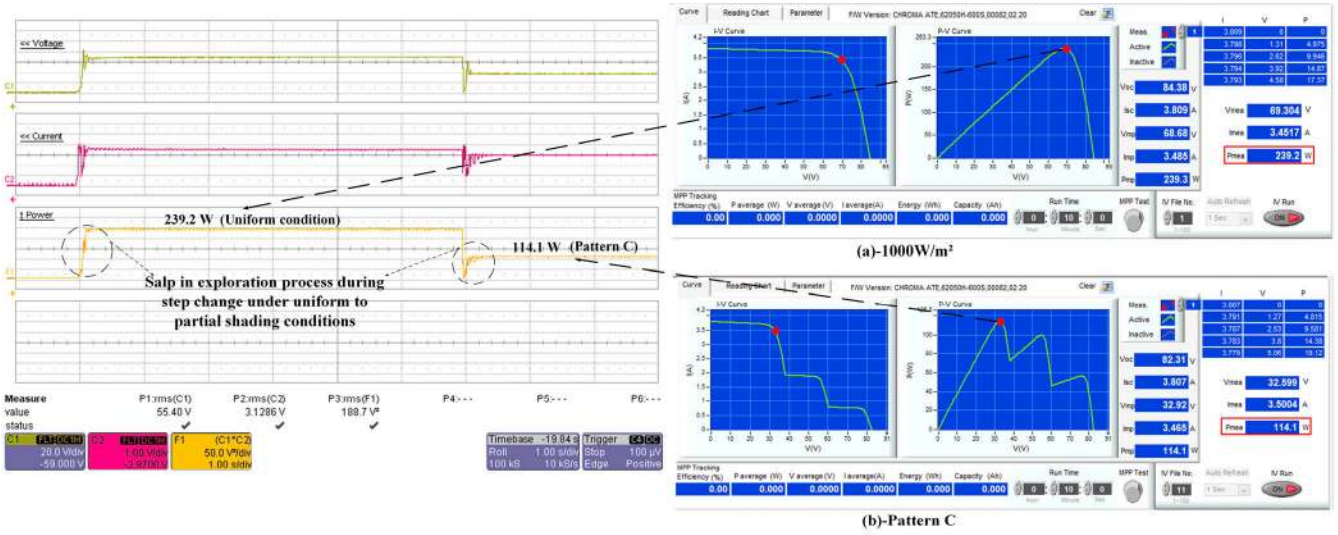

FIGURE 22. *I-V* and *P-V* curves under uniform conditions to PSCs (Pattern C).

MPP is less than 0.5 s, and the tracked power efficiency is 99.97%.

The final test is designed to validate the tracking performance during extreme dynamic environmental conditions. Initially, the *I-V* curve is uniform at 800 W/m^2. After 10 s, the condition changes to PS (*I-V* curve for pattern 2; see Fig. 29) and remains the same for 15 s before changing back to the uniform condition at 700 W/m^2. This test demonstrates the tracking effectiveness of the proposed SSA (Fig. 30).

The results reveal that the proposed SSA achieves the correct MPPs in all conditions. For the first condition, the GMPP (48.07 W) is reached within 0.2 s with an accuracy of 99.92%. When PS occurs (pattern 2, Fig. 29), the algorithm detects a change in power and initiates PS event checking based on Equation 6. The algorithm then decides that PS occurs and

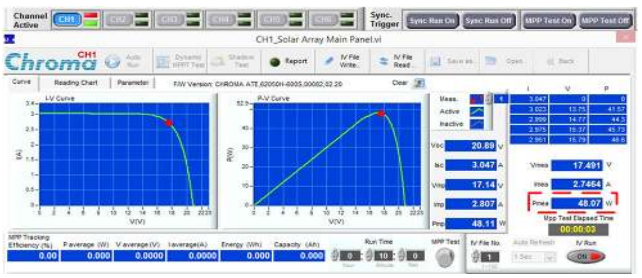

FIGURE 23. *I-V* and *P-V* curves under uniform conditions at irradiance of 800 W/m^2.

responds by reinitializing the search process. It randomly scans the *P-V* curve and converges to the GMPP at 23.69 W. The proposed SSA only takes 25 perturbations or around 0.5 s

TABLE 2. Performance and qualitative comparison of proposed SSA, conventional and metaheuristic method.

A. large step changes in uniform conditions						
Type	**HC**	**BOA**	**GWO**	**GOA**	**PSO**	**SSA**
Periodic Tuning	Not required	Required	Required	Required	Required	Required
Tracking Speed	Slow	Slow	Slow	Medium	Slow	Very Fast
Convergence Speed	Low	Slow	Slow	High	Slow	Very High
Sensed Parameters	V_{PV},I_{PV}	V_{PV},I_{PV}	V_{PV},I_{PV}	V_{PV},I_{PV}	V_{PV},I_{PV}	V_{PV},I_{PV}
Steady-state oscillations	Large	Zero	Zero	Zero	Zero	Zero
Dynamic Response	Good	Good	Good	Good	Good	Good
Tracking Accuracy	Low	High	High	High	High	Very High
Initial MPP tracking process	High Oscillation	High Oscillation	High Oscillation	High Oscillation	High Oscillation	Very Low Oscillation
B. large step changes in PSC						
Type	**HC**	**BOA**	**GWO**	**GOA**	**PSO**	**SSA**
Periodic Tuning	Not required	Required	Required	Required	Required	Required
Tracking Speed	Slow	Slow	Slow	Medium	Slow	Very Fast
Convergence Speed	Low (Trapped to local MPP)	Slow	Slow	High	Slow	Very High
Sensed Parameters	V_{PV},I_{PV}	V_{PV},I_{PV}	V_{PV},I_{PV}	V_{PV},I_{PV}	V_{PV},I_{PV}	V_{PV},I_{PV}
Steady-state oscillations	Large	Zero	Large	Zero	Zero	Zero
Dynamic Response	Good	Good	Very Low	Good	Good	Good
Tracking Accuracy	Low	Low	Very Low	Medium	Medium	Very High
Initial MPP tracking process	High Oscillation	High Oscillation	High Oscillation	High Oscillation	High Oscillation	Very Low Oscillation

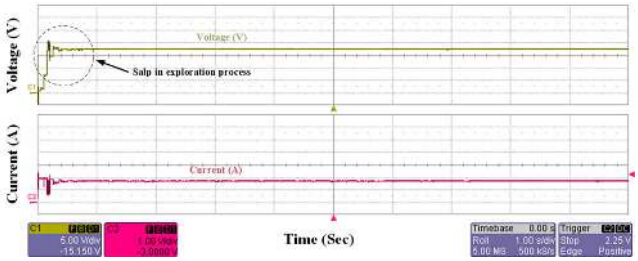

FIGURE 24. Current and voltage tracking responses for the SSA under static MPPT test (uniform condition at 800 W/m^2).

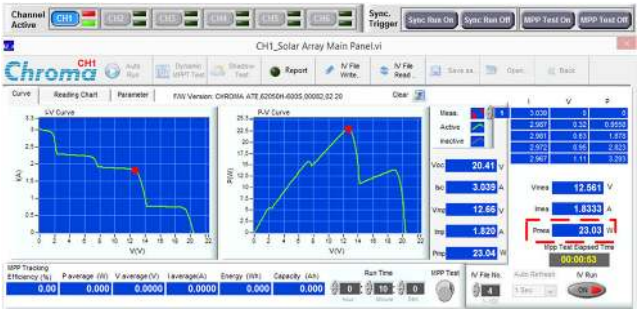

FIGURE 25. *I-V* and *P-V* curves under PSC for pattern 1.

to reach this point. After 15 s, uniform irradiance is restored at an irradiance of 700 W/m^2. Again, the algorithm detects a change in power and decides to restart the searching process. As the *P-V* curve only exhibits a single MPP, the algorithm is able to converge at the MPP within 0.22 s. The tracking accuracy at this point is 99.97% (42.18 W). The experimental results show good agreement with the simulations. For all the tested conditions, the MPP is achieved in a relatively short time. Hence, the superiority of the proposed algorithm is proved.

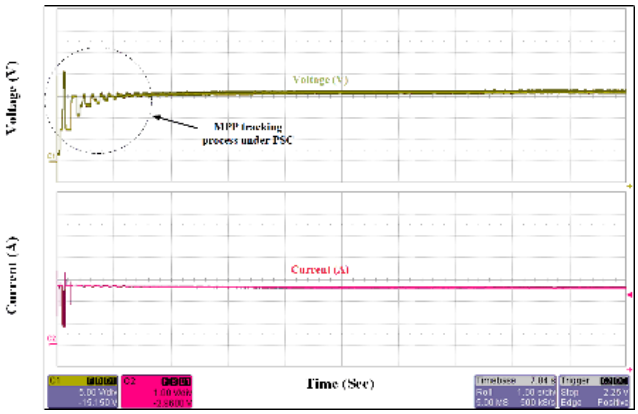

FIGURE 26. Current and voltage tracking responses for the SSA during PS.

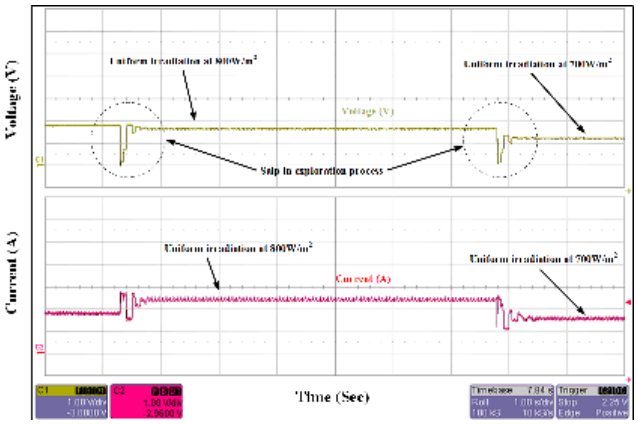

FIGURE 28. Current and voltage tracking responses for SSA during dynamic MPPT test (transition from 800 W/m^2 to 700 W/m^2).

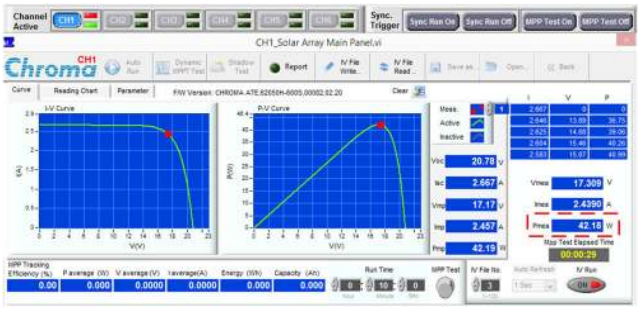

FIGURE 27. *I-V* and *P-V* curves under uniform conditions at an irradiance of 700 W/m^2.

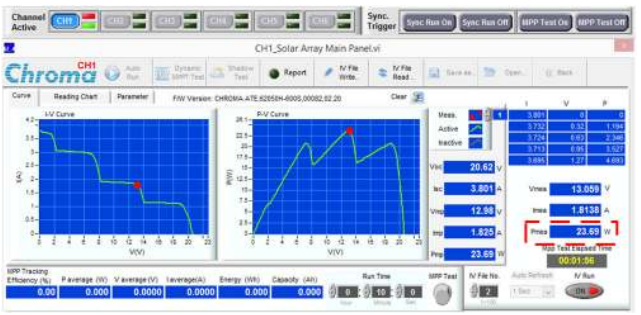

FIGURE 29. *I-V* and *P-V* curves under PSC for pattern 2.

VII. LIMITATION OF PROPOSED SSA

The main limitation of the proposed method and other metaheuristic-based algorithms is their ability to deal with a dynamic environment. The frequency of the environmental changes highly influences the probability of achieving global MPP. Thus, the algorithms that perform well on the static optimization problem could probably fail or give unsatisfactory results if they are directly implemented to deal with dynamic environments. For the MPPT problem with a very low frequency of irradiance changes, ample time is available for the algorithm to run and a considerable number of iterations can occur before the change is encountered, hence increasing the chance of those global optima being achieved. Contrarily, for the high frequency of changes, where time is the limitation, very few iterations can occur. Thus, it reduces the probability of the GMPP to be reached by the algorithm.

Another limitation of the proposed algorithm is the information on the severity of change in fitness landscapes (*P-V* curve) before and after the change has occurred is not considered during the tracking process. As a result, the algorithm has not used the information gathered from the previous landscape and must re-initialize and restart the new MPP search. This aspect could be improved if the pre-change fitness landscape information can be re-utilized in the post-change fitness landscape. For small changes that have low

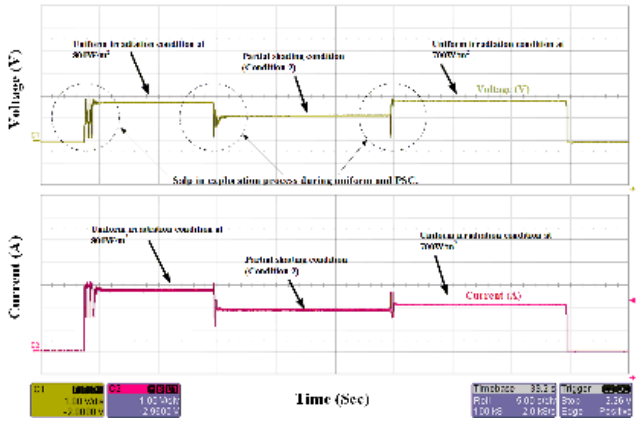

FIGURE 30. Current and voltage tracking responses for SSA under transition from uniform condition (800 W/m^2) to PSC (pattern 2) and uniform condition (700 W/m^2).

severity, the *P-V* curve transformation keeps the new MPP in the vicinity of old GMPP locations. Therefore, the algorithm can exploit the information from previous positions of MPP to locate and achieve the new global MPP. If the changes are small and ample information can be re-utilized, the algorithm may recover from the change in a short span. By doing so, the tracking performance, especially during a gradual change in irradiance can be significantly improved.

VIII. CONCLUSION

The SSA–MPPT technique is proposed in this work to track the MPP of a PV system at various environmental conditions. The proposed SSA can track the GMPP efficiently under dynamic irradiance conditions, including PS. The proposed algorithm's key merits are its ability to deal with dynamic MPPT problems with a straightforward structure and its only needs few steps to track the real MPP. The results reveal that the proposed SSA outperforms HC and other popular metaheuristics algorithms in all aspects, particularly in terms of tracking speed and accuracy. The simulation and hardware results also clarify the algorithm's superiority in terms of its average efficiency of around 99% under various environmental conditions. The proposed algorithm is expected to attract PV researchers and professionals seeking an efficient PV system operation.

ACKNOWLEDGMENT

The opinions, findings and conclusions or recommendations expressed in this material are those of the authors and do not necessarily reflect the views of the Science Foundation Ireland.

REFERENCES

[1] Á.-A. Bayod-Rújula and J.-A. Cebollero-Abián, "A novel MPPT method for PV systems with irradiance measurement," *Sol. Energy*, vol. 109, pp. 95–104, Nov. 2014.

[2] Y.-Y. Hong, A. A. Beltran, and A. C. Paglinawan, "A robust design of maximum power point tracking using taguchi method for stand-alone PV system," *Appl. Energy*, vol. 211, pp. 50–63, Feb. 2018.

[3] B. Yang, L. Zhong, X. Zhang, H. Shu, T. Yu, H. Li, L. Jiang, and L. Sun, "Novel bio-inspired memetic salp swarm algorithm and application to MPPT for PV systems considering partial shading condition," *J. Cleaner Prod.*, vol. 215, pp. 1203–1222, Apr. 2019.

[4] M. A. Danandeh and S. M. Mousavi, "Comparative and comprehensive review of maximum power point tracking methods for PV cells," *Renew. Sustain. Energy Rev.*, vol. 82, pp. 2743–2767, Feb. 2018.

[5] M. H. Taghvaee, M. A. M. Radzi, S. M. Moosavain, H. Hizam, and M. H. Marhaban, "A current and future study on non-isolated DC-DC converters for photovoltaic applications," *Renew. Sustain. Energy Rev.*, vol. 17, pp. 216–227, 2013.

[6] R. Boukenoui, H. Salhi, R. Bradai, and A. Mellit, "A new intelligent MPPT method for stand-alone photovoltaic systems operating under fast transient variations of shading patterns," *Sol. Energy*, vol. 124, pp. 124–142, Feb. 2016.

[7] R. Ahmad, A. F. Murtaza, and H. A. Sher, "Power tracking techniques for efficient operation of photovoltaic array in solar applications—A review," *Renew. Sustain. Energy Rev.*, vol. 101, pp. 82–102, Mar. 2019.

[8] T. S. Babu, N. Rajasekar, and K. Sangeetha, "Modified particle swarm optimization technique based maximum power point tracking for uniform and under partial shading condition," *Appl. Soft Comput.*, vol. 34, pp. 613–624, Sep. 2015.

[9] N. Rajasekar, M. Vysakh, H. V. Thakur, S. M. Azharuddin, K. Muralidhar, D. Paul, B. Jacob, K. Balasubramanian, and T. S. Babu, "Application of modified particle swarm optimization for maximum power point tracking under partial shading condition," *Energy Procedia*, vol. 61, pp. 2633–2639, 2014.

[10] E. Kabalci, "Maximum power point tracking (MPPT) algorithms for photovoltaic systems," in *Energy Harvesting and Energy Efficiency*. Cham, Switzerland: Springer, 2017, pp. 205–234.

[11] J. P. Ram and N. Rajasekar, "A novel flower pollination based global maximum power point method for solar maximum power point tracking," *IEEE Trans. Power Electron.*, vol. 32, no. 11, pp. 8486–8499, Nov. 2017.

[12] D. Yousri, S. B. Thanikanti, K. Balasubramanian, A. Osama, and A. Fathy, "Multi-objective grey wolf optimizer for optimal design of switching matrix for shaded PV array dynamic reconfiguration," *IEEE Access*, vol. 8, no. 2020, pp. 159931–159946.

[13] D. Yousri, T. S. Babu, S. Mirjalili, N. Rajasekar, and M. A. Elaziz, "A novel objective function with artificial ecosystem-based optimization for relieving the mismatching power loss of large-scale photovoltaic array," *Energy Convers. Manage.*, vol. 225, Dec. 2020, Art. no. 113385.

[14] B. Bendib, H. Belmili, and F. Krim, "A survey of the most used MPPT methods: Conventional and advanced algorithms applied for photovoltaic systems," *Renew. Sustain. Energy Rev.*, vol. 45, pp. 637–648, May 2015.

[15] J. P. Ram, T. S. Babu, and N. Rajasekar, "FPA based approach for solar maximum power point tracking," in *Proc. IEEE 6th Int. Conf. Power Syst. (ICPS)*, Mar. 2016, pp. 1–6.

[16] N. A. Kamarzaman and C. W. Tan, "A comprehensive review of maximum power point tracking algorithms for photovoltaic systems," *Renew. Sustain. Energy Rev.*, vol. 37, pp. 585–598, Sep. 2014.

[17] A. I. M. Ali, M. A. Sayed, and E. E. M. Mohamed, "Modified efficient perturb and observe maximum power point tracking technique for grid-tied PV system," *Int. J. Electr. Power Energy Syst.*, vol. 99, pp. 192–202, Jul. 2018.

[18] K. Sangeetha, T. S. Babu, and N. Rajasekar, "Fireworks algorithm-based maximum power point tracking for uniform irradiation as well as under partial shading condition," in *Artificial Intelligence and Evolutionary Computations in Engineering Systems*. New Delhi, India: Springer, 2016, pp. 79–88.

[19] K. Soon Tey and S. Mekhilef, "Modified incremental conductance algorithm for photovoltaic system under partial shading conditions and load variation," *IEEE Trans. Ind. Electron.*, vol. 61, no. 10, pp. 5384–5392, Oct. 2014.

[20] V. R. Kota and M. N. Bhukya, "A novel linear tangents based P&O scheme for MPPT of a PV system," *Renew. Sustain. Energy Rev.*, vol. 71, pp. 257–267, Mar. 2017.

[21] B. N. Alajmi, K. H. Ahmed, S. J. Finney, and B. W. Williams, "Fuzzy-logic-control approach of a modified hill-climbing method for maximum power point in microgrid standalone photovoltaic system," *IEEE Trans. Power Electron.*, vol. 26, no. 4, pp. 1022–1030, Apr. 2011.

[22] T. Radjai, L. Rahmani, S. Mekhilef, and J. P. Gaubert, "Implementation of a modified incremental conductance MPPT algorithm with direct control based on a fuzzy duty cycle change estimator using dSPACE," *Sol. Energy*, vol. 110, pp. 325–337, Dec. 2014.

[23] T. Esram, J. W. Kimball, P. T. Krein, P. L. Chapman, and P. Midya, "Dynamic maximum power point tracking of photovoltaic arrays using ripple correlation control," *IEEE Trans. Power Electron.*, vol. 21, no. 5, pp. 1282–1290, Sep. 2006.

[24] H. Heydari-Doostabad, R. Keypour, M. R. Khalghani, and M. H. Khooban, "A new approach in MPPT for photovoltaic array based on extremum seeking control under uniform and non-uniform irradiances," *Sol. Energy*, vol. 94, pp. 28–36, Aug. 2013.

[25] Y.-T. Chen, Y.-C. Jhang, and R.-H. Liang, "A fuzzy-logic based auto-scaling variable step-size MPPT method for PV systems," *Sol. Energy*, vol. 126, pp. 53–63, Mar. 2016.

[26] S. A. Rizzo and G. Scelba, "ANN based MPPT method for rapidly variable shading conditions," *Appl. Energy*, vol. 145, pp. 124–132, May 2015.

[27] L. Bouselham, M. Hajji, B. Hajji, and H. Bouali, "A new MPPT-based ANN for photovoltaic system under partial shading conditions," *Energy Procedia*, vol. 111, pp. 924–933, Mar. 2017.

[28] R. Ramaprabha, V. Gothandaraman, K. Kanimozhi, R. Divya, and B. L. Mathur, "Maximum power point tracking using GA-optimized artificial neural network for solar PV system," in *Proc. 1st Int. Conf. Electr. Energy Syst.*, no. 1, Jan. 2011, pp. 264–268.

[29] J. Shi, W. Zhang, Y. Zhang, F. Xue, and T. Yang, "MPPT for PV systems based on a dormant PSO algorithm," *Electr. Power Syst. Res.*, vol. 123, pp. 100–107, Jun. 2015.

[30] K. Ishaque, Z. Salam, M. Amjad, and S. Mekhilef, "An improved particle swarm optimization (PSO)–based MPPT for PV with reduced steady-state oscillation," *IEEE Trans. Power Electron.*, vol. 27, no. 8, pp. 3627–3638, Aug. 2012.

[31] J. Ahmed and Z. Salam, "A maximum power point tracking (MPPT) for PV system using cuckoo search with partial shading capability," *Appl. Energy*, vol. 119, pp. 118–130, Apr. 2014.

[32] D. Yousri, T. S. Babu, D. Allam, V. K. Ramachandaramurthy, E. Beshr, and M. B. Eteiba, "Fractional chaos maps with flower pollination algorithm for partial shading mitigation of photovoltaic systems," *Energies*, vol. 12, no. 18, p. 3548, Sep. 2019.

[33] T. S. Babu, D. Yousri, and K. Balasubramanian, "Photovoltaic array reconfiguration system for maximizing the harvested power using population-based algorithms," *IEEE Access*, vol. 8, pp. 109608–109624, 2020.

[34] S. Krishnan G, S. Kinattingal, S. P. Simon, and P. S. R. Nayak, "MPPT in PV systems using ant colony optimisation with dwindling population," *IET Renew. Power Gener.*, vol. 14, no. 7, pp. 1105–1112, May 2020.
[35] K. Aygül, M. Cikan, T. Demirdelen, and M. Tumay, "Butterfly optimization algorithm based maximum power point tracking of photovoltaic systems under partial shading condition," *Energy Sources A, Recovery, Utilization, Environ. Effects*, Oct. 2019, pp. 1–9.
[36] I. Shams, S. Mekhilef, and K. S. Tey, "Maximum power point tracking using modified butterfly optimization algorithm for partial shading, uniform shading, and fast varying load conditions," *IEEE Trans. Power Electron.*, vol. 36, no. 5, pp. 5569–5581, May 2021.
[37] M. Mansoor, A. F. Mirza, Q. Ling, and M. Y. Javed, "Novel grass hopper optimization based MPPT of PV systems for complex partial shading conditions," *Sol. Energy*, vol. 198, pp. 499–518, Mar. 2020.
[38] A. M. Eltamaly, M. S. Al-Saud, and A. G. Abokhalil, "A novel bat algorithm strategy for maximum power point tracker of photovoltaic energy systems under dynamic partial shading," *IEEE Access*, vol. 8, pp. 10048–10060, Dec. 2020.
[39] M. Premkumar, T. S. Babu, S. Umashankar, and R. Sowmya, "A new metaphor-less algorithms for the photovoltaic cell parameter estimation," *Optik*, vol. 208, Apr. 2020, Art. no. 164559.
[40] K. L. Lian, J. H. Jhang, and I. S. Tian, "A maximum power point tracking method based on perturb-and-observe combined with particle swarm optimization," *IEEE J. Photovolt.*, vol. 4, no. 2, pp. 626–633, Mar. 2014.
[41] K. Ishaque and Z. Salam, "A deterministic particle swarm optimization maximum power point tracker for photovoltaic system under partial shading condition," *IEEE Trans. Ind. Electron.*, vol. 60, no. 8, pp. 3195–3206, May 2012.
[42] G. Shankar and V. Mukherjee, "MPP detection of a partially shaded PV array by continuous GA and hybrid PSO," *Ain Shams Eng. J.*, vol. 6, no. 2, pp. 471–479, Jun. 2015.
[43] J. P. Ram and N. Rajasekar, "A new global maximum power point tracking technique for solar photovoltaic (PV) system under partial shading conditions (PSC)," *Energy*, vol. 118, pp. 512–525, Jan. 2017.
[44] M. Kermadi, Z. Salam, J. Ahmed, and E. M. Berkouk, "A high-performance global maximum power point tracker of PV system for rapidly changing partial shading conditions," *IEEE Trans. Ind. Electron.*, vol. 68, no. 3, pp. 2236–2245, Mar. 2021.
[45] S. Mohanty, B. Subudhi, and P. K. Ray, "A new MPPT design using grey wolf optimization technique for photovoltaic system under partial shading conditions," *IEEE Trans. Sustain. Energy*, vol. 7, no. 1, pp. 181–188, Jan. 2016.
[46] D. F. Teshome, C. H. Lee, Y. W. Lin, and K. L. Lian, "A modified firefly algorithm for photovoltaic maximum power point tracking control under partial shading," *IEEE J. Emerg. Sel. Topics Power Electron.*, vol. 5, no. 2, pp. 661–671, Jun. 2017.
[47] D. Yousri, S. B. Thanikanti, D. Allam, V. K. Ramachandaramurthy, and M. B. Eteiba, "Fractional chaotic ensemble particle swarm optimizer for identifying the single, double, and three diode photovoltaic models' parameters," *Energy*, vol. 195, Mar. 2020, Art. no. 116979.
[48] O. Abdalla, H. Rezk, and E. M. Ahmed, "Wind driven optimization algorithm based global MPPT for PV system under non-uniform solar irradiance," *Sol. Energy*, vol. 180, pp. 429–444, Mar. 2019.
[49] K. S. Tey, S. Mekhilef, H.-T. Yang, and M.-K. Chuang, "A differential evolution based MPPT method for photovoltaic modules under partial shading conditions," *Int. J. Photoenergy*, vol. 2014, pp. 1–10, May 2014.
[50] S. Hadji, J.-P. Gaubert, and F. Krim, "Theoretical and experimental analysis of genetic algorithms based MPPT for PV systems," *Energy Procedia*, vol. 74, pp. 772–787, Aug. 2015.
[51] L. Guo, Z. Meng, Y. Sun, and L. Wang, "A modified cat swarm optimization based maximum power point tracking method for photovoltaic system under partially shaded condition," *Energy*, vol. 144, pp. 501–514, Feb. 2018.
[52] H. Yatimi and E. Aroudam, "Assessment and control of a photovoltaic energy storage system based on the robust sliding mode MPPT controller," *Sol. Energy*, vol. 139, pp. 557–568, Dec. 2016.
[53] M. Kermadi, V. J. Chin, S. Mekhilef, and Z. Salam, "A fast and accurate generalized analytical approach for PV arrays modeling under partial shading conditions," *Sol. Energy*, vol. 208, pp. 753–765, Sep. 2020.
[54] M. Joisher, D. Singh, S. Taheri, D. R. Espinoza-Trejo, E. Pouresmaeil, and H. Taheri, "A hybrid evolutionary-based MPPT for photovoltaic systems under partial shading conditions," *IEEE Access*, vol. 8, pp. 38481–38492, 2020.
[55] C. H. Basha and C. Rani, "Different conventional and soft computing MPPT techniques for solar PV systems with high step-up boost converters: A comprehensive analysis," *Energies*, vol. 13, no. 2, p. 371, Jan. 2020.
[56] J. P. Ram, D. S. Pillai, A. M. Y. M. Ghias, and N. Rajasekar, "Performance enhancement of solar PV systems applying P&O assisted flower pollination algorithm (FPA)," *Sol. Energy*, vol. 199, pp. 214–229, Feb. 2020.
[57] L. Avila, M. De Paula, M. Trimboli, and I. Carlucho, "Deep reinforcement learning approach for MPPT control of partially shaded PV systems in smart grids," *Appl. Soft Comput.*, vol. 97, Dec. 2020, Art. no. 106711.
[58] N. Priyadarshi, S. Padmanaban, J. B. Holm-Nielsen, F. Blaabjerg, and M. S. Bhaskar, "An experimental estimation of hybrid ANFIS–PSO-based MPPT for PV grid integration under fluctuating sun irradiance," *IEEE Syst. J.*, vol. 14, no. 1, pp. 1218–1229, Mar. 2020.
[59] J. S. Goud, R. Kalpana, B. Singh, and S. Kumar, "Maximum power point tracking technique using artificial bee colony and hill climbing algorithms during mismatch insolation conditions on PV array," *IET Renew. Power Gener.*, vol. 12, no. 16, pp. 1915–1922, Dec. 2018.
[60] N. Priyadarshi, S. Padmanaban, P. K. Maroti, and A. Sharma, "An extensive practical investigation of FPSO-based MPPT for grid integrated PV system under variable operating conditions with anti-islanding protection," *IEEE Syst. J.*, vol. 13, no. 2, pp. 1861–1871, Jun. 2019.
[61] D. Pilakkat and S. Kanthalakshmi, "An improved P&O algorithm integrated with artificial bee colony for photovoltaic systems under partial shading conditions," *Sol. Energy*, vol. 178, pp. 37–47, Mar. 2019.
[62] M. Mao, L. Zhou, Z. Yang, Q. Zhang, C. Zheng, B. Xie, and Y. Wan, "A hybrid intelligent GMPPT algorithm for partial shading PV system," *Control Eng. Pract.*, vol. 83, pp. 108–115, Feb. 2019.
[63] M. Seyedmahmoudian, R. Rahmani, S. Mekhilef, A. M. T. Oo, A. Stojcevski, T. K. Soon, and A. S. Ghandhari, "Simulation and hardware implementation of new maximum power point tracking technique for partially shaded PV system using hybrid DEPSO method," *IEEE Trans. Sustain. Energy*, vol. 6, no. 3, pp. 850–862, Jul. 2015.
[64] S. Mirjalili, A. H. Gandomi, S. Z. Mirjalili, S. Saremi, H. Faris, and S. M. Mirjalili, "Salp swarm algorithm: A bio-inspired optimizer for engineering design problems," *Adv. Eng. Softw.*, vol. 114, pp. 163–191, Dec. 2017.
[65] Y. Liu, S. Huang, J. Huang, and W. Liang, "A particle swarm optimization-based maximum power point tracking algorithm for PV systems," *IEEE Trans. Energy Convers.*, vol. 27, no. 4, pp. 1027–1035, Oct. 2012.

MOHD NASRUL IZZANI JAMALUDIN received the B.Eng. degree in electrical engineering from Universiti Teknologi Malaysia (UTM), Malaysia, in 2003, and the M.Sc. degree in electrical power engineering from Universiti Malaysia Perlis (UniMAP), Malaysia, in 2016. He is currently pursuing the Ph.D. degree in electrical engineering with the Faculty of Electrical Engineering Technology, UniMAP. His research interests include power electronics, photovoltaic systems, maximum power point tracking techniques, and optimization algorithms.

MOHAMMAD FARIDUN NAIM TAJUDDIN received the B.Eng. and M.Eng. degrees from the University of Malaya (UM), Malaysia, in 2004 and 2007 respectively, and the Ph.D. degree from the Universiti Teknologi Malaysia (UTM), Malaysia, in 2015. He is currently with the Faculty of Electrical Engineering Technology, Universiti Malaysia Perlis (UniMAP). He has published refereed manuscripts in various reputable international journals. His research interests include power electronics control, photovoltaic modeling and control, intelligent control, and optimization techniques. He is also acting as a Reviewer for various reputed journals, such as the IEEE, *Applied Energy* (Elsevier), *Renewable and Sustainable Energy Reviews*, *Neurocomputing*, and *Energy Reports*.

JUBAER AHMED (Member, IEEE) received the B.Sc. degree in electrical and electronics engineering from the Bangladesh University of Engineering and Technology, Dhaka, Bangladesh, in 2012, and the Ph.D. degree in electrical engineering from Universiti Teknologi Malaysia, Johor Bahru, Malaysia, in 2016. He is currently a Lecturer with the Swinburne University of Technology Sarawak, Kuching, Malaysia. His research interests include photovoltaic modeling and control, energy conversion from renewable sources, and power electronics

AZRALMUKMIN AZMI (Member, IEEE) received the B.Eng. degree (Hons.) in electrical system engineering from the University Malaysia Perlis (UniMAP), in 2007, and the M.Eng. degree in electrical-power from Universiti Teknologi Malaysia (UTM), in 2009. He is currently a Lecturer with the Faculty of Electrical Engineering Technology, UniMAP. His research interests include artificial intelligence and optimization, power systems, power electronics, high voltage, and renewable energy.

SYAHRUL ASHIKIN AZMI received the B.Sc. degree from the PETRONAS University of Technology, Malaysia, in 2003, the M.Sc. degree from the University of New South Wales, Australia, in 2004, and the Ph.D. degree from the University of Strathclyde, Glasgow, U.K., in 2014. She is currently with the Faculty of Electrical Engineering Technology, Universiti Malaysia Perlis (UniMAP). Her research interests include digital control of power electronic systems, microgrids, distributed generation, and power quality.

NUR HAFIZAH GHAZALI (Member, IEEE) received the B.Sc. degree from Universiti Teknologi Malaysia (UTM), Malaysia, in 2006, the M.Sc. degree from Universiti Utara Malaysia (UUM), Malaysia, in 2010, and the Ph.D. degree from UTM, in 2015. She is currently with the Faculty of Electronic Engineering, Universiti Malaysia Perlis (UniMAP). Her research interests include artificial intelligence, optimization algorithms, image processing, and data hiding.

THANIKANTI SUDHAKAR BABU (Senior Member, IEEE) received the B.Tech. degree from Jawaharlal Nehru Technological University, Anantapur, India, in 2009, the M.Tech. degree in power electronics and industrial drives from Anna University, Chennai, India, in 2011, and the Ph.D. degree from VIT University, Vellore, India, in 2017.

He worked as an Assistant Professor senior with the School of Electrical Engineering, VIT University. He is currently working as an Associate Professor with the Department of Electrical Engineering, Chaitanya Bharathi Institute of Technology (CBIT), Hyderabad, India. He had completed his Postdoctoral Researcher Fellowship with the Institute of Power Engineering, Universiti Tenaga Nasional (UNITEN), Malaysia. He has published more than 60 research articles in various renowned international journals. His research interests include the design and implementation of solar PV systems, renewable energy resources, power management for hybrid energy systems, storage systems, fuel cell technologies, electric vehicles, and smart grids. He has been acting as an Editorial Board Member and a Reviewer for various reputed journals, such as the IEEE and IEEE Access, IET, Elsevier, and Taylor and Francis.

HASSAN HAES ALHELOU (Senior Member, IEEE) is currently a Senior Researcher with UCD. He is also a Faculty Member with Tishreen University, Lattakia, Syria. He has participated in more than 15 industrial projects. He has published more than 100 research articles in the high quality peer-reviewed journals and international conferences. His major research interests include power systems, power system dynamics, power system operation and control, dynamic state estimation, frequency control, smart grids, micro-grids, demand response, load shedding, and power system protection. In 2018 and 2019, he included Publons list of the Top 1% Best Reviewer and Researchers in the field of engineering. He was a recipient of the Outstanding Reviewer Award from the *Energy Conversion and Management* Journal, in 2016, ISA *Transactions Journal*, in 2018, *Applied Energy* Journal, in 2019, the Best Young Researcher Award with the Arab Student Forum Creative among 61 researchers from 16 countries by Alexandria University, Egypt, 2011. He has also performed more than 600 reviews for high prestigious journals, including IEEE Transactions on Industrial Informatics, IEEE Transactions on Industrial Electronics, Energy Conversion and Management, *Applied Energy*, *International Journal of Electrical Power and Energy Systems*.